CONFIDENTIAL

VLF EARTH-CURRENT COMMUNICATION
INTERIM REPORT

27 October 1960

50X1

50X1

CONFIDENTIAL

50X1
50X1

TABLE OF CONTENTS

SECTION I - SUMMARY

SECTION II - SURFACE WAVE PROPAGATION

SECTION III - CONDUCTING LAYER PROPAGATION

APPENDICES

50X1

LIST OF ILLUSTRATIONS

50X1
50X1

LIST OF ILLUSTRATIONS (Continued)

LIST OF TABLES

550X1

LIST OF TABLES (Continued)

50X1

SECTION I

SUMMARY

1.1 SUMMARY

This report covers the application of earth current communication techniques to a portable communications equipment for operation over ranges from 2 to 300 miles. Propagation and noise characteristics are considered for frequencies up to 100 kc.

1.1.1 Surface Wave Propagation (Horizontal Electrode Spacing)

Using data rates of about 5 words per minute, a pocket-sized set can communicate at ranges from 3 to 30 miles, depending upon noise conditions. A larger battery-powered set weighting 150 lbs. total (in two or three portable cases) has a range from about 15 to 700 miles, depending upon frequency and noise conditions. Even under high noise conditions, the 150 lb. set can communicate at 80 words per minute to a range of 55 miles. A frequency of 100 kc results in the most advantageous propagation characteristics, but such equipment could readily be detected and jammed, even at relatively long ranges. For ranges less than 10 miles, frequencies on the order of 100 cps and lower are advantageous. Jamming at long range would be virtually impossible with such a system. For longer ranges, frequencies of 3 kc or 30 kc are applicable, with 3 kc having shorter range capability but greater resistance to jamming.

1.1.2 Conducting Layer Propagation (Vertical Electrode Spacing)

Using a data rate of about 5 words per minute, a pocket-sized set can communicate at ranges from about 4 to 8 miles, depending upon noise. The larger 150 lb. set can similarly communicate from about 10 to 18 miles at 5 wpm. At 80 wpm the corresponding figures are about 2 to 3 miles and 4 to 8 miles, respectively. Frequencies of around 1 kc and less are advantageous, and the system is extremely resistant to jamming.

50X1

SECTION II

SURFACE WAVE PROPAGATION

2.1   INTRODUCTION

This section is concerned with the application of surface earth current communication techniques for two-way communication over ranges from 2 to 300 miles, between a central fixed station and portable field station.

A typical earth current transmitter feeds current into two electrodes buried in the earth. The resulting electromagnetic field propagates along the surface of the earth where it can be received by appropriate detection equipment. Receiving equipment can use either horizontal antennas (electrodes buried in the earth) or vertical antennas. Horizontal electrode antennas pick up a smaller signal but result in the same signal-to-noise ratio. A wave similar to that generated by earth current equipment could be launched by a vertical antenna; but, such an antenna would be very tall and conspicuous and extremely vulnerable to attack. For these reasons it seems appropriate that both transmitter and receiver use earth electrode type antennas.

The signal strength is proportional to both electrode current (I) and electrode current (L). For the purpose of this report it is assumed that a maximum electrode separation of 100 meters can be used with portable equipment. For a given transmitter power, current can be maximized by minimizing the impedance (using large electrodes). Where a permanent deep electrode installation can be made, it is possible to achieve an electrode earth resistance of an ohm or less. For a portable station, however, it has been assumed that no buried conductors (such as water pipes) are available, and that earth contact is made by means of two iron pipes about 5 feet long driven into the earth about 100 meters apart. When the stakes are set in typical soil and the area around them is wet, an impedance of about 50 ohms results - this value being assumed throughout this section. However, when a buried conductor such as a water well casing or water main is available to serve as one electrode, the total resistance may become much less than 50 ohms, and the same transmitter power would then result in a signal improvement of about 10 db per decade reduction of electrode impedance over that assumed in this analysis.

An artist's conception of a portable earth current field station for transmitting and receiving is shown in Figure 1. The central station would be similar, except that it would be permanently housed, and thus could use permanent electrodes having a lower impedance.
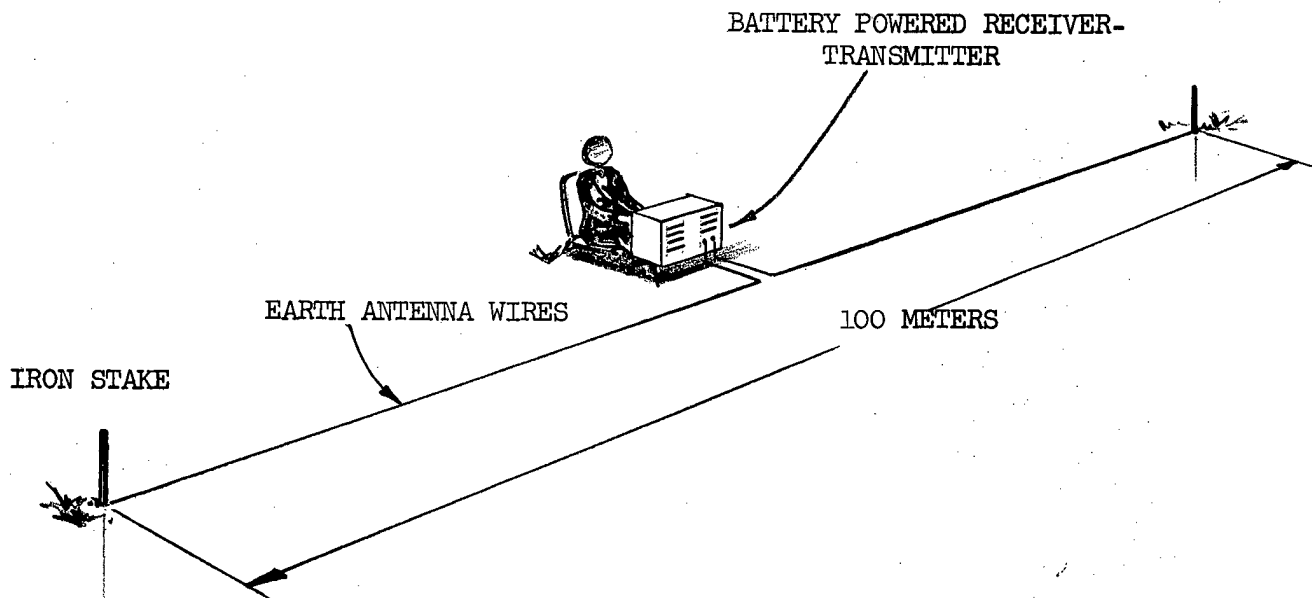
FIGURE 1. Portable Earth Current Communication Equipment

50X1

2.2   SURFACE WAVE PROPAGATION AT LOW FREQUENCIES

When both transmitting and receiving electrodes are located at the surface of a homogeneous earth, the horizontal electric field at the receiving electrode is given by[1]:

$$E\rho = \frac{IL}{2\pi^2 \sigma \rho^3} \left| 1 - \left(\frac{2\pi\rho}{\lambda}\right)^2 + j \left(\frac{2\pi\rho}{\lambda}\right) \right| \tag{1}$$

where I is the current in amperes

L is the electrode separation in meters

σ is the conductivity

ρ is the range in meters

λ is the wavelength in air

It can be seen that for small values of ρ/λ, the field drops off as inverse range cubed.

At longer ranges, however, the term on the right begins to be important, until at long range this term becomes equal to $\left(\frac{2\pi\rho}{\lambda}\right)^2$, and the field becomes

$$E\rho \cong \frac{IL}{2\pi\sigma\rho^3} \left[\frac{2\pi\rho}{\lambda}\right]^2 \qquad \rho/\lambda >> 1 \tag{2}$$

Thus, at long ranges, the field is proportional to inverse range. A plot of

$$\left| 1 - \left(\frac{2\pi\rho}{\lambda}\right)^2 + j \left(\frac{2\pi\rho}{\lambda}\right) \right|$$

is shown in Figure 2. The break point occurs at $\rho/\lambda \cong 0.16$. Using the first equation, the field can be plotted as a function of range for a given transmitter power. Thus for 5000 watts, $I = 10$ amperes into 50 ohms. Then, using $L = 100$ meters and $\sigma = 10^{-2}$ mho/meter, the field can be computed from the equation.

---

[1] A. Banos and J. P. Wesley: "The Horizontal Electric Dipole In A Conducting Half-Space", University of California Report S10 - Reference 53-33, to Bureau of Ships, September, 1953.

50X1

80

70

60

50

40

30

DECIBELS

20

10

0

0.16 = $\frac{\rho}{\lambda}$

-10

-20

-30

-40

.02   0.05   0.1 $\frac{\rho}{\lambda}$ 1   10

Page 7

FIGURE 2. Plot of $\left| 1 - \left(\frac{2\pi\rho}{\lambda}\right)^2 + j \ \frac{2\pi\rho}{\lambda} \right|$ In Decibels

This procedure is good for frequencies up to about 30 kc. At 100 kc, however, an earth current antenna of 100 meter length (consisting of a wire lain along the ground and two electrodes) reaches resonance, resulting in a high resistive component of impedance, thus severely limiting the current for a given power. Also, the current distribution along the wire becomes non-un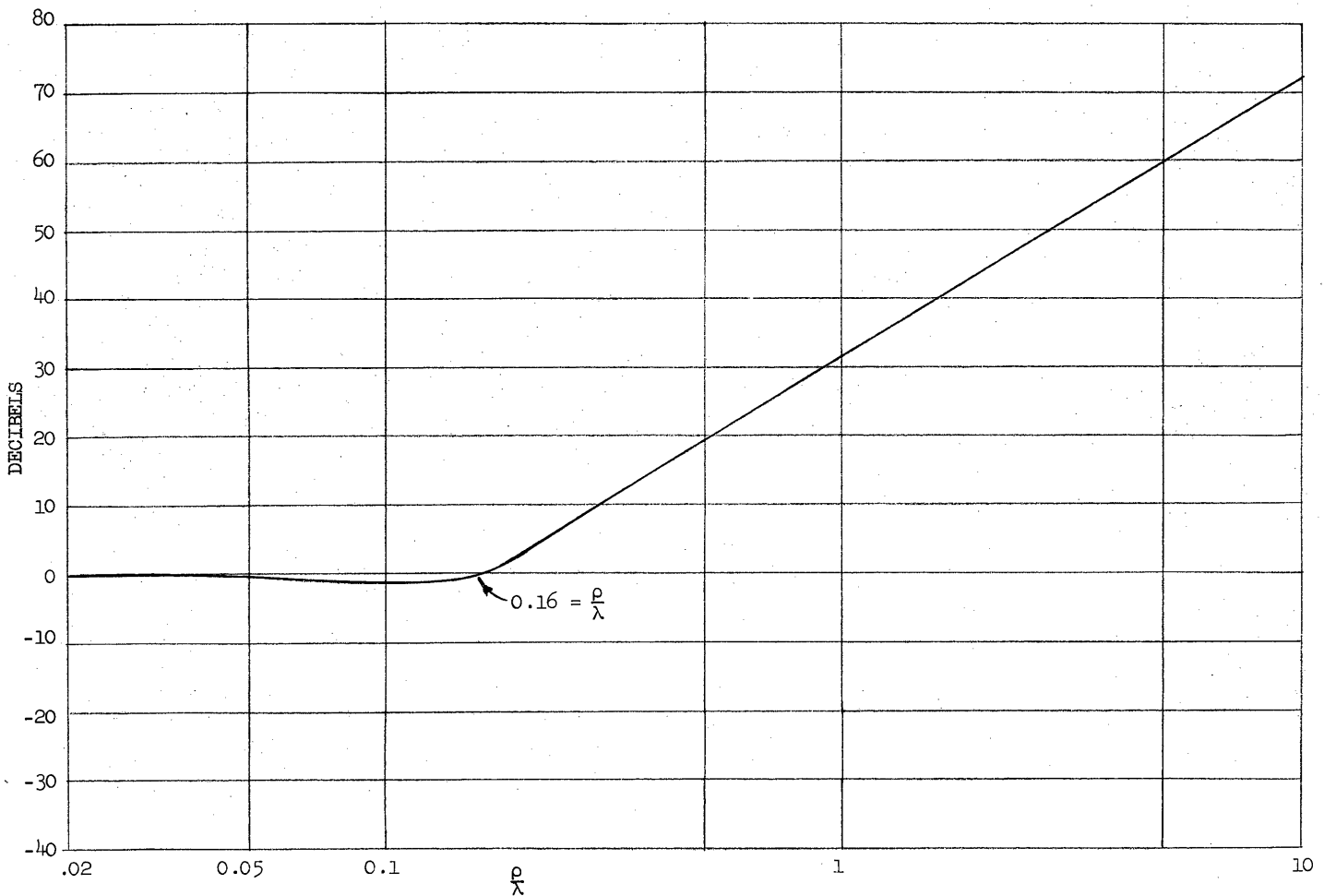iform. At 100 kc it would be more advantageous to use a 50 meter length and thus avoid resonance. The antenna impedance would then be the same as at lower frequencies (i.e., 50 ohms). Thus only 6 db (due to shortening L) is lost. Also, at 100 kc the curvature of the earth becomes important at long ranges and causes the field to decay somewhat faster than inverse range. This effect[2] has been taken into account in the 100 kc case. Effects of the ionosphere begin to be important also at very long range. However, at the 300-mile maximum range requirement in this study, such effects can be neglected. Figure 3 gives a plot of equation (1) for frequencies of 1 kc, 3 kc, 10 kc, and 30 kc for a power of 5000 watts (current of 10 amperes) with a 100 meter antenna. Figure 4 gives a plot for the 100 kc case, including a 6 db loss (using a 50 meter antenna) and greater attenuation at long range due to the curvature of the earth.

2.3   SURFACE LAYER PROPAGATION AT ULTRA LOW FREQUENCIES

The conductivity of the outer earth's crust varies widely among the many materials of which it is composed. Sea water has a conductivity of about 4 mhos/meter, while gneiss and granite of pre-Cambrian age have conductivities as low as 10^{-5} mho/meter. The surface of the earth typically has a conductivity of about 10^{-2} mho/meter. The geologically older material at greater depths usually has considerably smaller conductivity. In some areas, particularly where sedimentary formations exist, alternating layers of low and highly conducting material may occur. A typical condition, however, is that in which a weathered surface layer of relatively shallow depth, and having a high conductivity, overlays a geologically older, denser, and less conductive material. At high frequencies, the skin depth may be so shallow that appreciable current does not penetrate to the lower layer, in which case the earth current propagation characteristics may be determined from the usual analysis for a homogeneous earth. When the surface layer depth is appreciably less than a skin depth in the upper medium, then the effect of the lower

---

[2]Terman: Radio Engineer's Handbook.
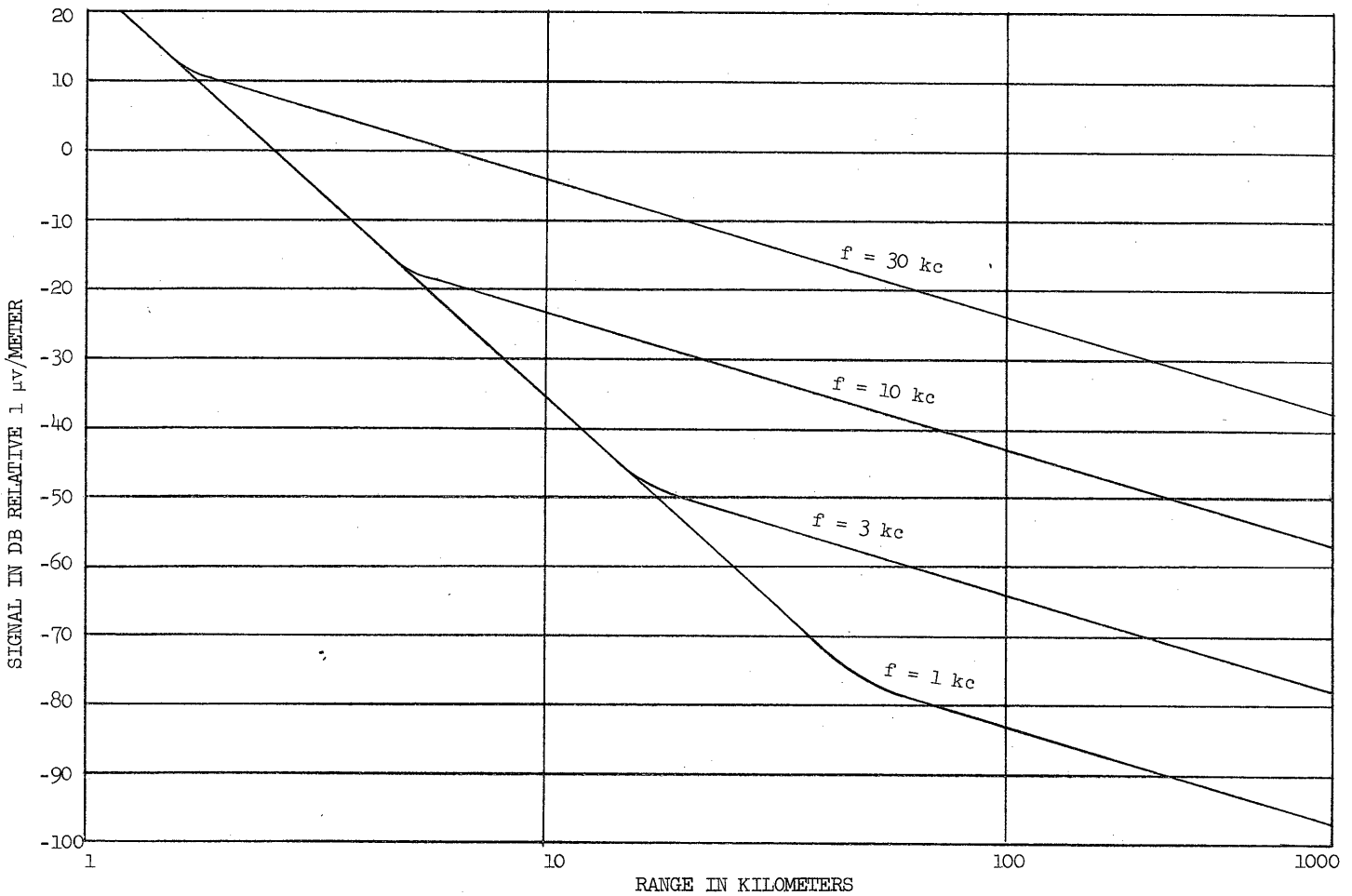
FIGURE 3.   Signal Strength vs Range, 1 to 30 kc
For I = 10 Amperes,   L = 100 Meters
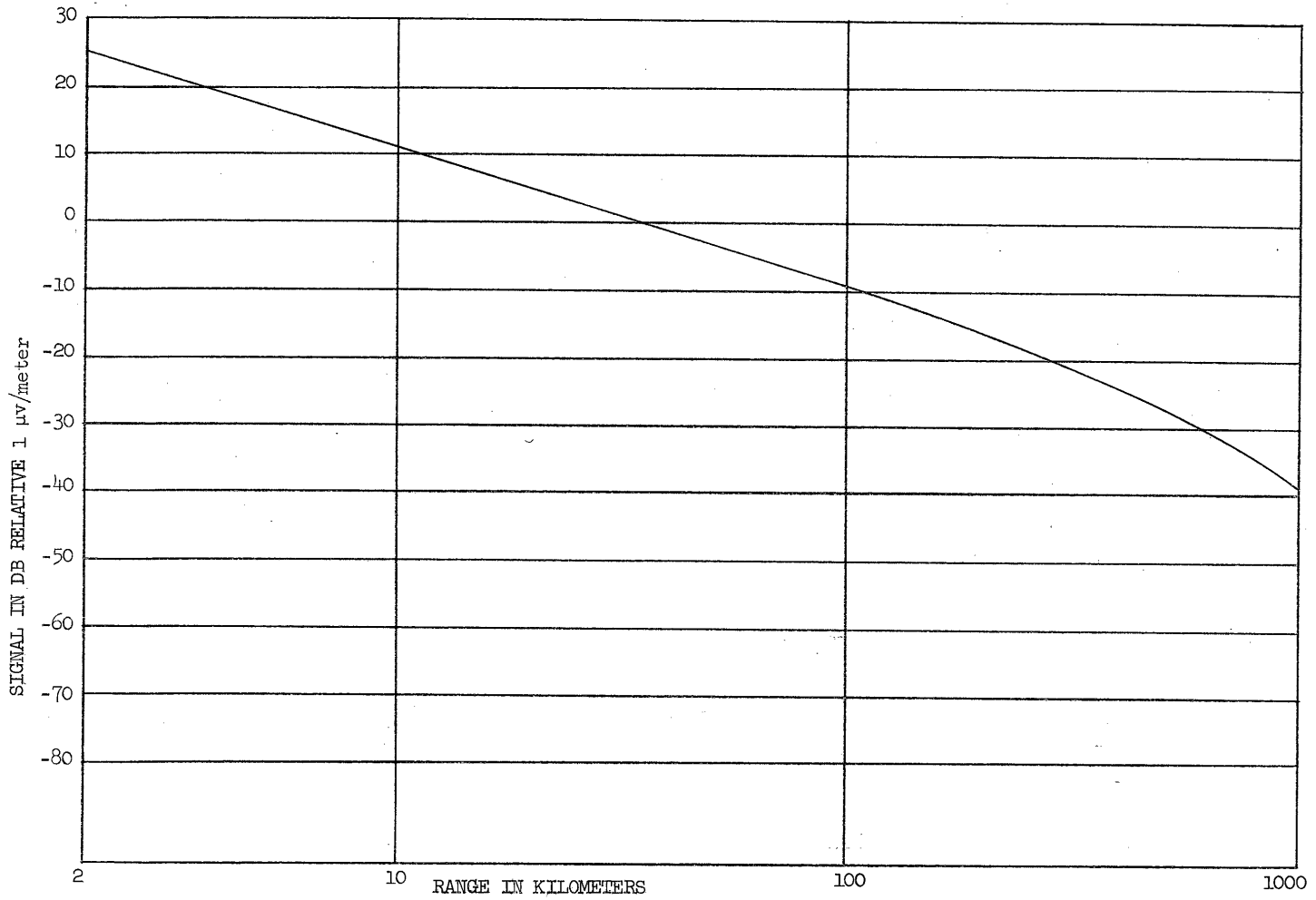
FIGURE 4. Signal Strength vs Range, f = 100 kc
For I = 10 Amperes, L = 50 Meters

medium must be taken into account in the analysis. A useful approximation is obtained from an analysis of the static case (i.e., from the d-c current case). The condition of interest is diagrammed in Figure 5, where the surface layer has conductivity σ_1, and the basement material has conductivity σ_2. The transmitter electrodes are spaced a distance L, and carry current I. The depth of the layer is d, and ρ is the distance from transmitter to receiver. The radial component of the electric field at the surface of the earth is then given by[3]:

$$E_\rho = \left[\frac{IL}{\pi \sigma_1 d^3}\right] \cdot E_{\rho_0} \qquad E_{\rho_0} \text{ in volts per meter}$$

where E_{ρ_0} is a dimensionless quantity given by

$$E_{\rho_0} = \frac{1}{y^3} \left\{ 1 + \int_{1/2}^{\infty} \frac{\left[2 - \left(\frac{2x}{y}\right)^2\right] \alpha^x}{\left[1 + \left(\frac{2x}{y}\right)^2\right]^{5/2}} \, dx \right\}$$

where $y = \dfrac{\rho}{d}$

$$\alpha = \frac{\sigma_1 - \sigma_2}{\sigma_1 + \sigma_2} \quad .$$

When $\sigma_1 = \sigma_2$, then $\alpha = 0$ and the solution reduces to

$$E_\rho = \frac{IL}{\pi \sigma_1 \rho^3}$$

which is the solution for a homogeneous earth in the d-c case. A plot of E_{ρ_0} in decibels is given in Appendix A as a function of the quantity

$$y = \frac{\rho}{d} \quad .$$

---

[3] cf. Appendix A.
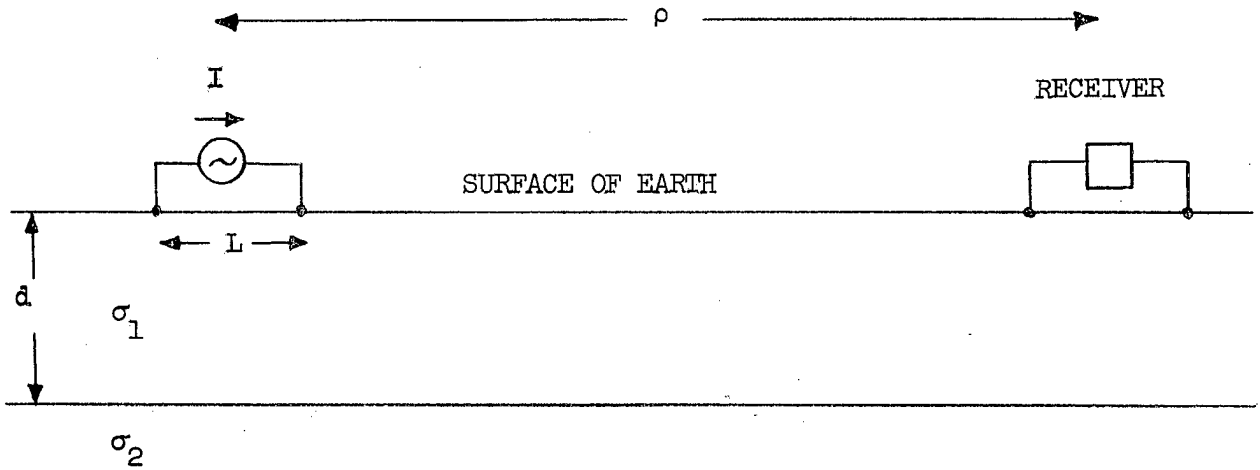
FIGURE 5.   Two Layer Earth

When $\sigma_2 < \sigma_1$ (i.e., when the lower material is less conducting), then E_ρ is greater than in the case of the homogeneous earth, as can be seen from the figure. Three layer depths d which are chosen for study are 10, 100, and 1000 meters. These cover the range of typical conducting layer depths. Also it was assumed that

$$\sigma_1 = 10^{-2} \text{ mho/meter}$$
$$I = 10 \text{ amperes (5000 watts into 50 ohms)}$$
$$L = 100 \text{ meters.}$$

The resulting curves of E_ρ vs. range in kilometers were plotted in Figures 6, 7, and 8. The curves are plotted for three values of σ_2/σ_1 (i.e., $\sigma_2/\sigma_1 = 1$, 0.1, and 0.01). The curve for $\sigma_2/\sigma_1 = 1$ represents the d-c case for a homogeneous earth. Although the graphs are plotted for a 5000 watt input, they are readily transformable to any power input at the rate of 10 db loss in signal per decade reduction in power.

The curves shown, while derived on a d-c basis, should form a good approximation to the propagation of earth current energy out to ranges not exceeding about 0.16 wavelength in air, provided the skin depth δ is greater than the layer depth d. Skin depth δ and wavelength λ are plotted in Figure 9 as a function of frequency, for $\sigma_1 = 10^{-2}$ mho/meter. At a frequency of 10 cps, $\delta = 1600$ meters; at 100 cps, $\delta = 500$ meters; and at 1000 cps, $\delta = 160$ meters, for $\sigma_1 = 10^{-2}$ mho/meter. Thus when the layer depth is 1000 meters, the presence of the lower material has little or no effect at frequencies much above 10 cps since then the skin depth is less than the layer depth. When the layer depth is 100 meters, the layer has effect out to a little above 100 cps, and thus the curves shown are applicable.

2.4 NOISE CHARACTERISTICS

The chief source of noise in the usual earth current communication system is atmospheric in origin. Atmospheric noise arises chiefly from lightning discharge, where the predominantly vertical current stroke results in a large
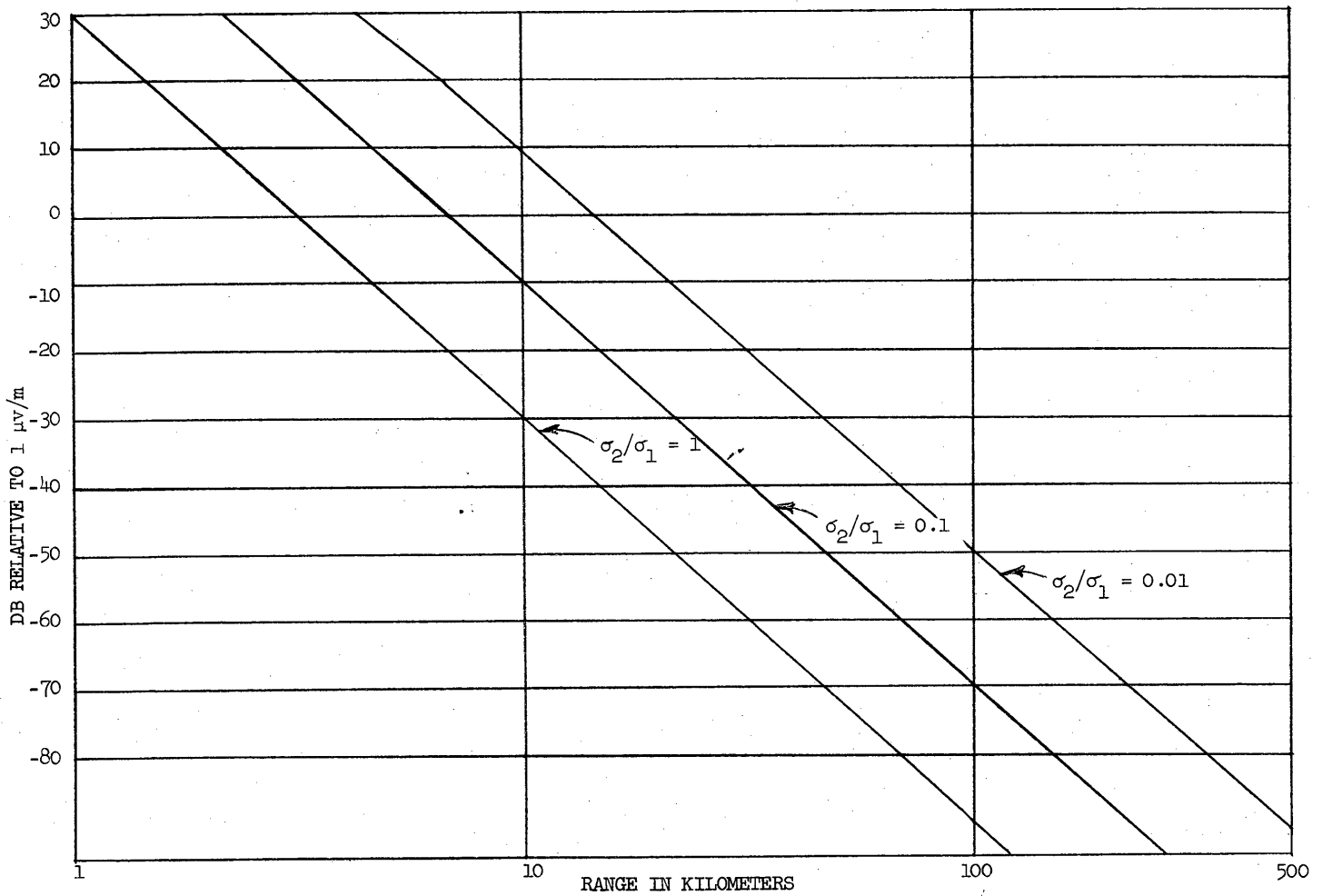
FIGURE 6. E_ρ vs. Range, d = 10 Meters

I = 10 Amperes
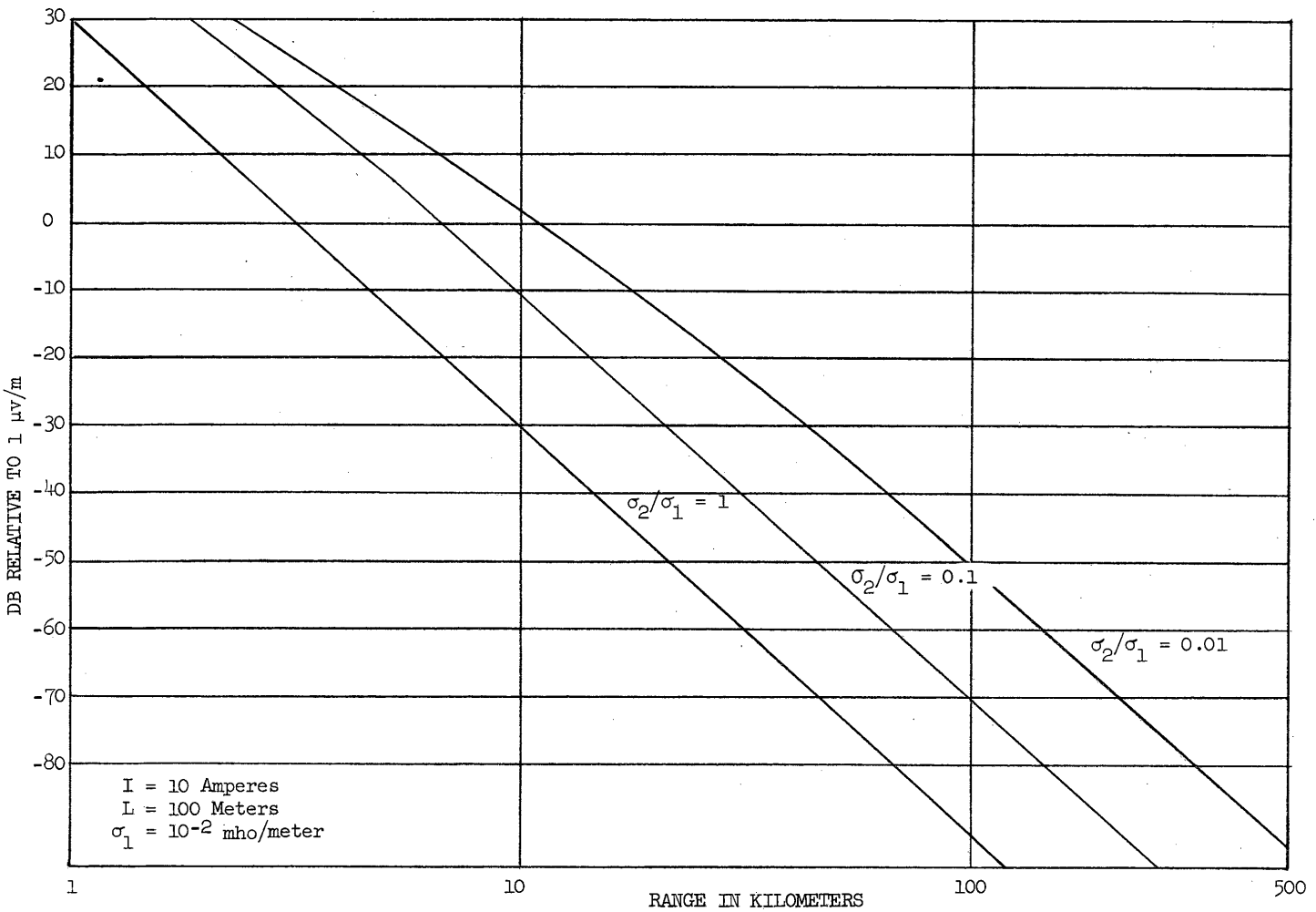
50X1

FIGURE 7. E_ρ vs Range, d = 100 Meters

50X1

I   =   10 Amps.

L   =   1000 Meters

σ_1 =   0.01 mho/meter

d   =   1000 Meters

$\sigma_2/\sigma_1 = 0.01$

$\sigma_2/\sigma_1 = 1$ $\sigma_2/\sigma_1 = 0.1$

DB Relative to 1 $\mu v/m$

Range in Kilometers

Page 16
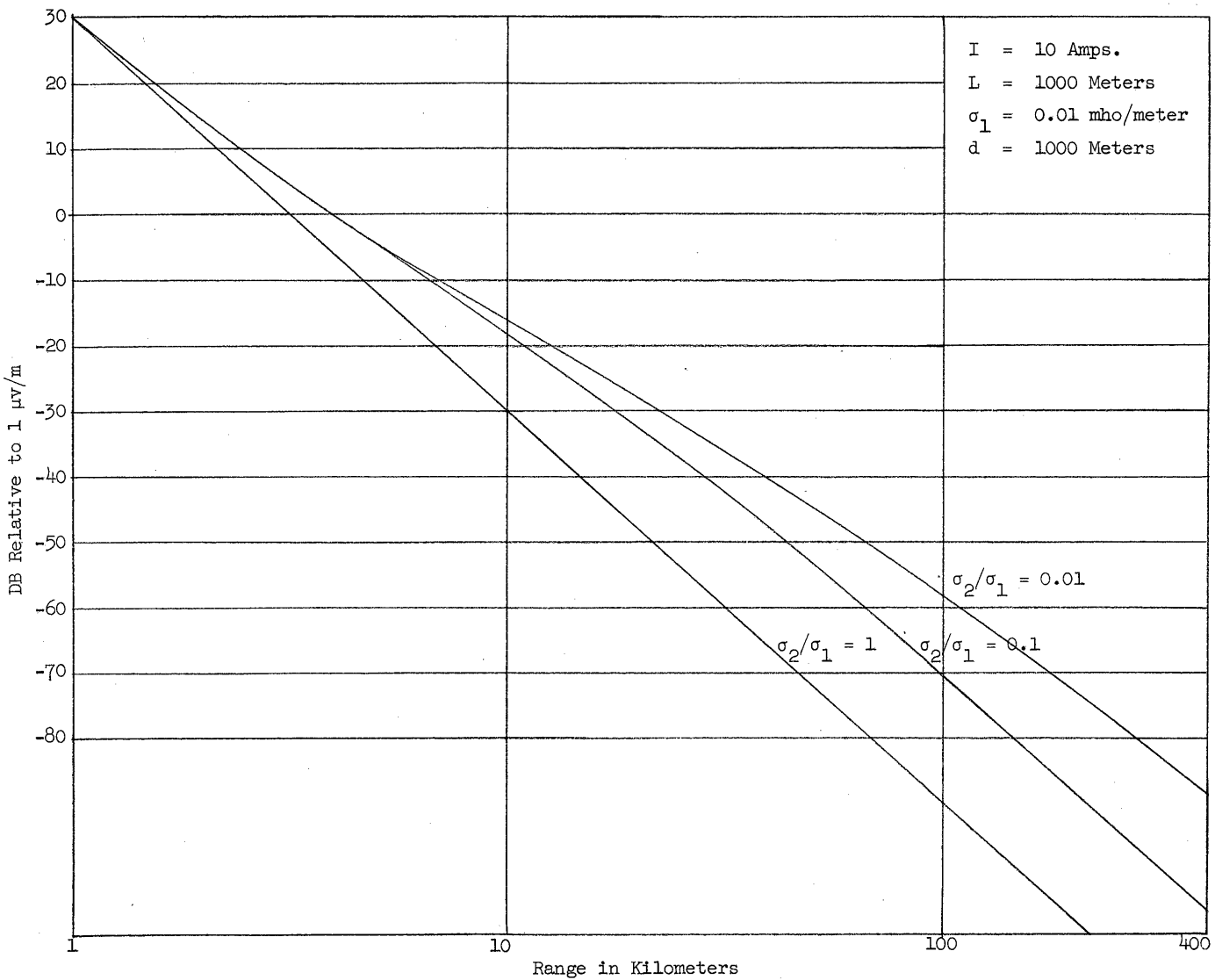
50X1
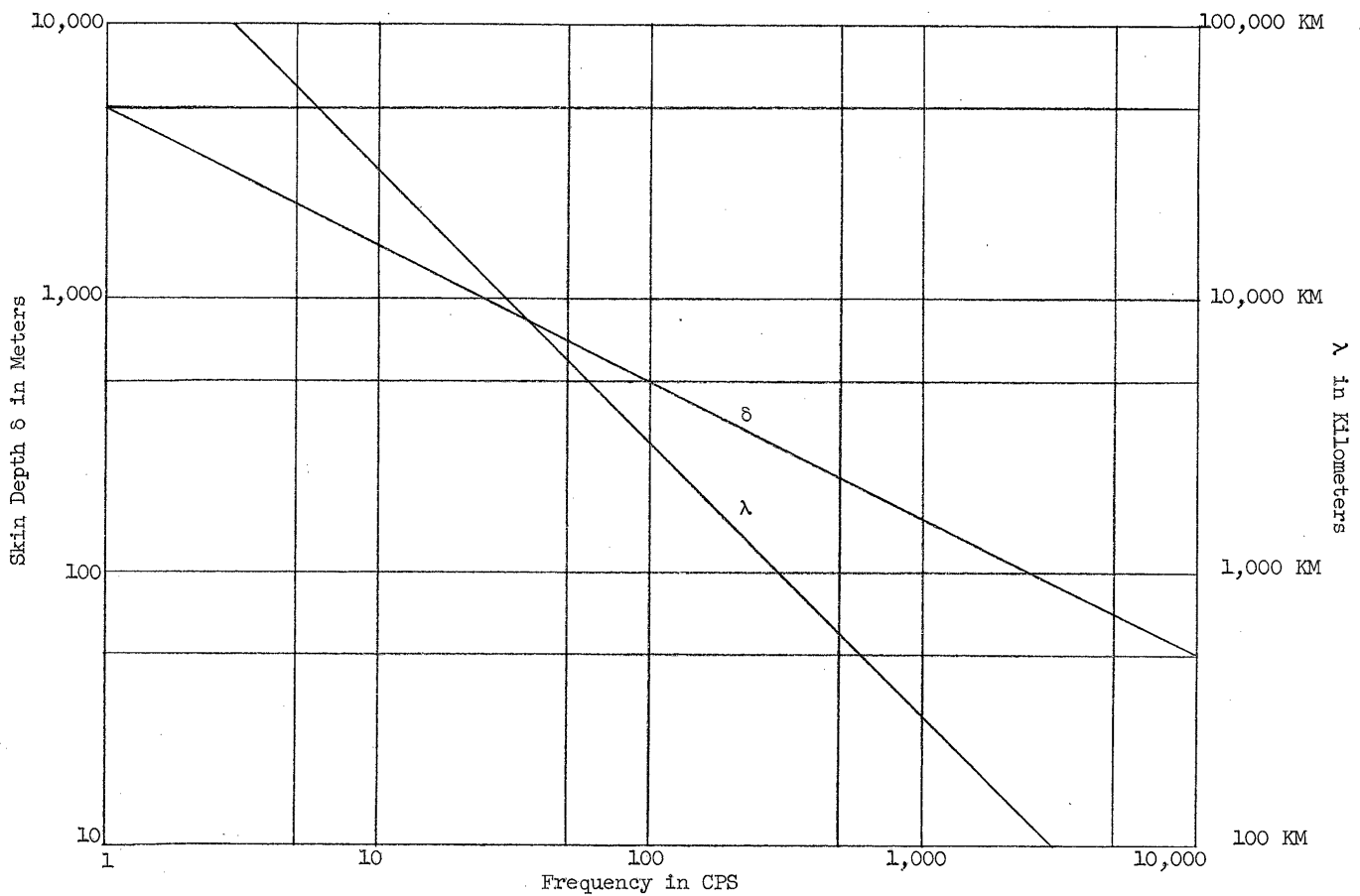
FIGURE 9.   Skin Depth δ and Air Wavelength λ vs Frequency

$$\sigma = 10^{-2} \, \text{mho/meter}$$

50X1

Page 18

radiated field. Such pulses have appreciable energy in the spectrum from a few cycles up to above 100 kc. The electric field in air is predominantly vertical, but the much slower phase velocity in the earth results in a predominantly horizontal field in the ground at the surface. The ratio of the vertical field in air to the horizontal field in the earth is large at low frequencies and is given by $\sqrt{\dfrac{\sigma}{\omega \, \xi_o}}$. This is plotted in Figure 10 for

$\sigma = 10^{-2}$ mho/meter. This ratio was used to convert noise measurements made in air to the applicable values for earth current receivers using electrode antennas. Measurements have also been made by

50X1

and others of the noise voltage between earth electrodes. A summary of such measurements is given in Figure 11. This figure shows the equivalent mean value of the noise envelope in a 1 cps bandwidth. The noise level can vary widely during a single day, and from season to season. There is a pronounced minimum of noise in the neighborhood of 3 kc. This minimum is predicted by the mode theory of VLF propagation[4] which shows greater attenuation, at ranges beyond about 500 miles, at these frequencies. At shorter ranges, the propagation at 3 kc follows the usual inverse range dependence. Thus the ionosphere, in the 3 kc range, operates to reduce the level of noise originating over 500 miles away more than that at other frequencies. Applying the mode theory to the close-in measured spectra of lightning discharges gives long-range spectra whose shape agrees well with the measured values[5]. The fact that noise is low at 3 kc and that this frequency discriminates against jamming sources located 500 miles or more away makes 3 kc an attractive frequency for this application.

Recent tests by

have confirmed the theo-

50X1

retical propagation characteristics at 3 kc. High power was used in the tests, and when the measured data are scaled to the assumptions (i.e., I = 10 amps, L = 100 meters) used in this report, the measured values can be compared, as shown in Figure 12. The attenuation over the inverse range line is negligible for the ranges considered here for communication purposes (2 to 300 miles), and so is neglected in the analysis.

---

[4] cf. Proceedings of the IRE, June 1957.
[5] ibid.

50X1

$$\frac{E_V}{E_H} = \sqrt{\frac{\sigma}{\omega \, \epsilon_o}}$$

$\sigma = 10^{-2}$ mho/meter

Frequency in CPS

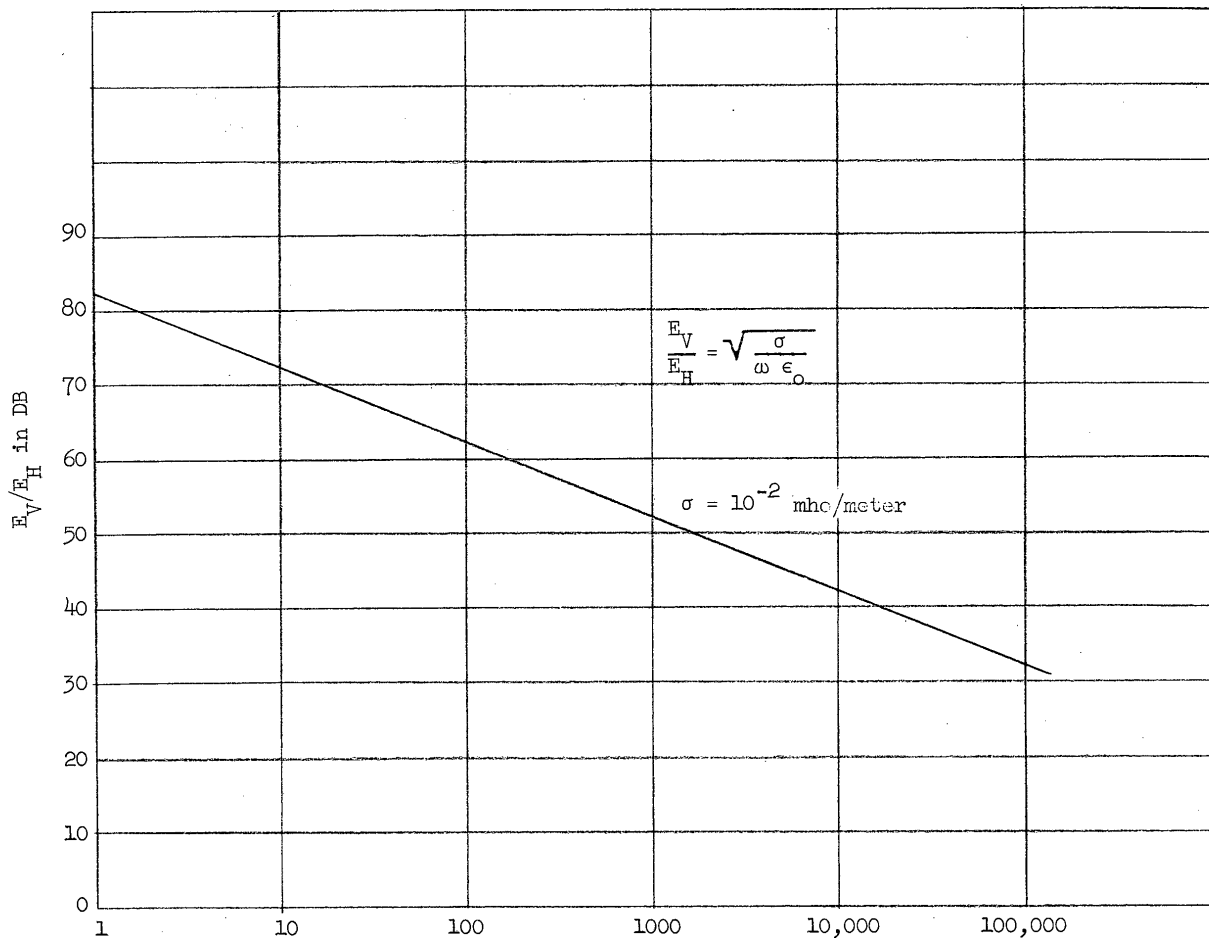FIGURE 10. Ratio E_V/E_H of Vertical Field in
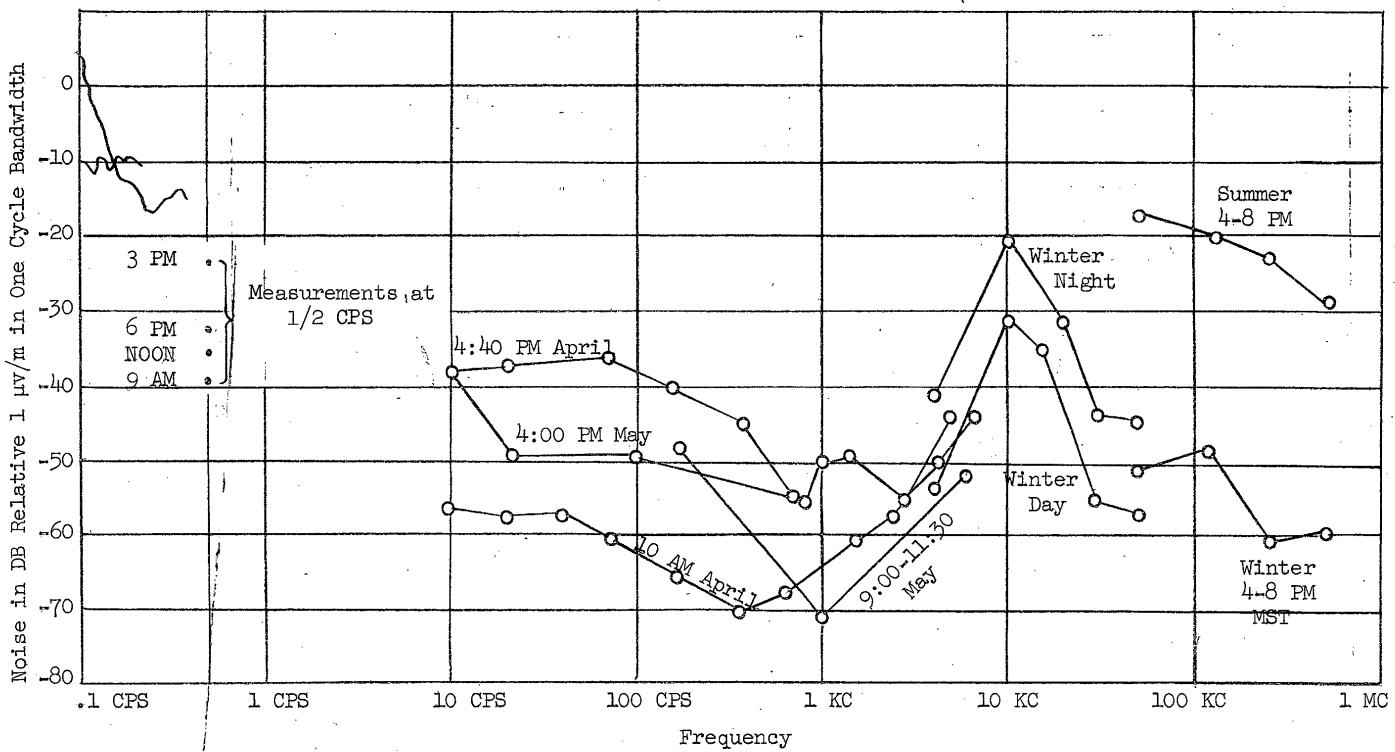Air to Horizontal Field in Earth

Page 19

50X1

FIGURE 11. Summary of Measurements of Horizontal Noise Field at Surface of Earth
(Mean Value of Noise Envelope for 1 CPS Bandwidth)
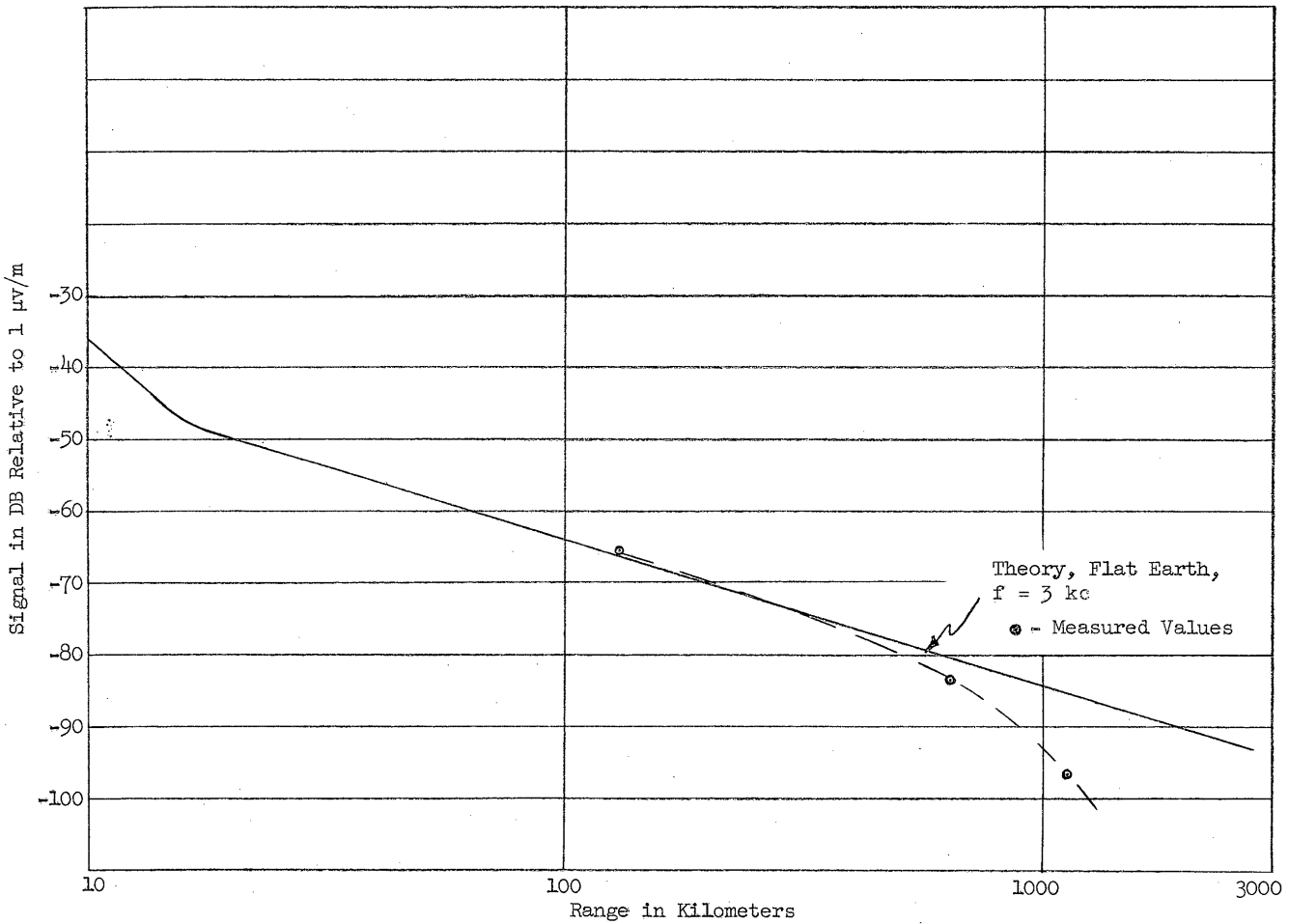
$$\sigma = 10^{-2} \text{ mho/meter}$$

50X1

FIGURE 12.   Comparison of Theoretical and Measured Signal at 3 kc

Page 21

For the purposes of this report, two standard noise spectra will be considered, as shown in Figure 13. The upper curve in the figure represents the "high" noise condition, or the value of noise exceeded roughly 10 percent of the time. The lower curve represents the "low" noise condition, or that value exceeded roughly 90 percent of the time.

The curves were drawn so as to represent reasonable noise conditions in the Western U.S. The "high" noise condition can be taken to represent a rough diurnal maximum noise condition. The "low" noise condition can be taken to represent the diurnal minimum. Thus if the communication system must work at any time on short notice, the "high" noise condition would be assumed. If, on the other hand, the operator can choose the time of day to send his message, then the "low" noise curve can be used. In the subsequent analysis, both noise conditions are considered and included in the determination of maximum range.

2.5   COMMUNICATION RANGE

The range to which a transmitter-receiver system can communicate depends upon the data rate and upon the signal/noise ratio at the receiver. If a S/N ratio of about 10 db is realized in a one cps bandwidth, then an information rate of two bits/second can be transmitted. If a 10 db S/N ratio is realized in a 4 cps bandwidth, then about 8 bits/second can be transmitted. Similarly, in a 16 cps bandwidth, 32 bits/second can be transmitted. Using optimum coding techniques, two bits/second carries a word rate of about 5 wpm.

Thus, if a system provides a 10 db S/N at 1 cps bandwidth, a 5 wpm data rate can be handled. If the bandwidth is widened to 4 cps, noise will be increased by 6 db. Thus, the signal must be increased by 6 db to provide a 20 wpm capability. Similarly, a 12 db increase would be necessary to realize 80 wpm capability with 16 cps bandwidth. The noise curves presented earlier are drawn for a 1 cps bandwidth. Then using these curves, the range at which a 10 db S/N ratio just occurs represents a maximum range for a 5 wpm capability. The range at which a 22 db S/N occurs represents 80 wpm, and 28 db S/N represents 320 wpm capability. These ranges were determined for both the high and the low noise condition, for powers of 1 watt and 5000 watts. At the lower frequencies ($f \leq 100$ cps) surface layers of 10, 100, and 1000 meters depth were used, corresponding to the propagation curves presented earlier. The results are given in Tables I, II, III and IV. The results are plotted in Figures 14, 15, 16 and 17, where a layer depth of 100 meters, and a conductivity ratio $\sigma_2/\sigma_1 = 0.1$ were assumed.

50X1
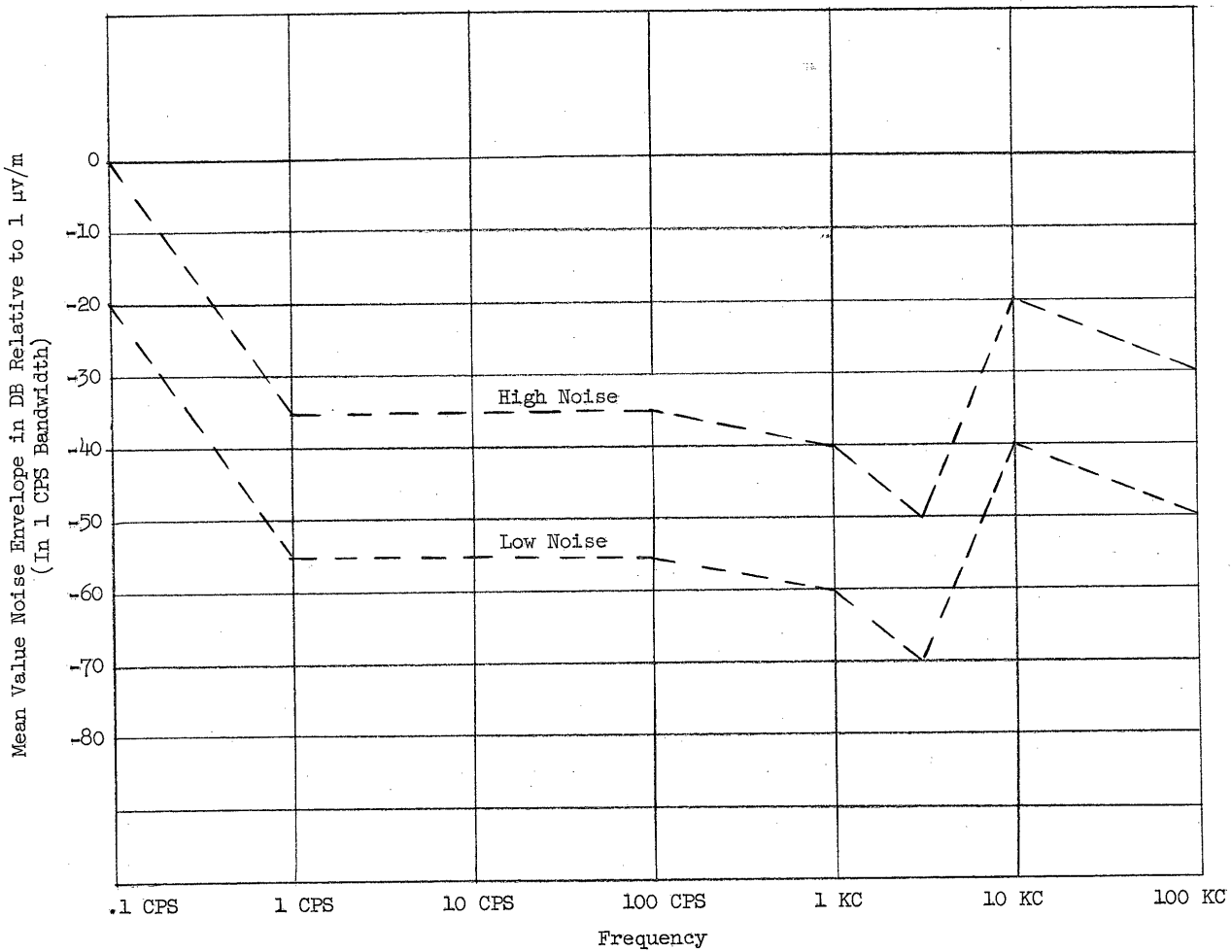
FIGURE 13. Standard Noise Spectra Used in Computation

Page 23

TABLE I

COMMUNICATION RANGE VS. FREQUENCY AND DATA RATE

LOW NOISE, 5000 WATTS POWER

50X1

Frequency	σ_2/σ_1	d (Meters)	5 WPM		20 WPM		80 WPM		320 WPM	
			KM	Miles	KM	Miles	KM	Miles	KM	Miles
100 cps	$\sigma_2/\sigma_1 = 1$		18	11.2	14	8.7	11	6.8		
	$\sigma_2/\sigma_1 = 0.1$	10	38	23.6	31	19.2	24	15		
		100	38	23.6	30	18.6	24	15		
		1000	35	21.8	27	16.8	20	12.4		
	$\sigma_2/\sigma_1 = 0.01$	10	83	51.5	66	41	52	32		
		100	80	49.7	64	39.7	48	30		
		1000	50	31	37	23	26	16		
1 kc			17	10.5	13.5	8.5	11	6.8	8.6	5.3
3 kc			63	39	31.5	19.5	16.5	10.3	12.6	7.8
10 kc			22	14	11	6.8	5.6	3.5	4	2.5
30 kc			360	220	180	112	90	56	45	28
100 kc			1100	683	780	484	520	323	330	205

50X1

(a) Bandwidth = 1 CPS (5 WPM)
(b) Bandwidth = 4 CPS (20 WPM)
(c) Bandwidth = 16 CPS (80 WPM)
(d) Bandwidth = 64 CPS (320 WPM)

RANGE IN MILES

FREQUENCY

FIGURE 14. Communication Range vs Frequency And Data Rate

(Low Noise, 5000 Watts, σ_2/σ_1 = 0.1, d = 100 Meters)

TABLE II

COMMUNICATION RANGE VS. FREQUENCY AND DATA RATE

HIGH NOISE, 5000 WATTS POWER

50X1

Frequency	σ_2/σ_1	d (Meters)	5 WPM		20 WPM		80 WPM		320 WPM	
			KM	Miles	KM	Miles	KM	Miles	KM	Miles
100 cps	$\sigma_2/\sigma_1 = 1$		8.2	5.1	6.6	4.1	5.2	3.2		
	$\sigma_2/\sigma_1 = 0.1$	10	18	11.2	14	8.7	11	6.8		
		100	18	11.2	14	8.7	11	6.8		
		1000	14	8.7	10.4	6.5	7.6	4.7		
	$\sigma_2/\sigma_1 = 0.01$	10	38	23.6	30	18.6	24	15		
		100	35	21.7	27	16.8	20	12.4		
		1000	17	10.5	12	7.5	8.3	5.1		
1 kc			7.9	4.9	6.4	4.0	5.0	3.1	4.0	2.5
3 kc			12	7.5	9.2	5.7	7.4	4.6	5.8	3.6
10 kc			3.7	2.3	2.9	1.8	2.3	1.4	1.86	1.15
30 kc			35	21.7	18	11.2	9.0	5.6	4.4	2.7
100 kc			280	174	160	99	90	56	46	29

50X1

(a) Bandwidth = 1 CPS (5 WPM)
(b) Bandwidth = 4 CPS (20 WPM)
(c) Bandwidth = 16 CPS (80 WPM)
(d) Bandwidth = 64 CPS (320 WPM)

RANGE IN MILES

FREQUENCY

Page 27

FIGURE 15. Communication Range vs Frequency And Data Rate
(High Noise, 5000 Watts, σ_{2}/σ_{1} = o.1, d = 100 Meters)

TABLE III

COMMUNICATION RANGE VS. FREQUENCY AND DATA RATE

50X1

LOW NOISE, 1 WATT POWER

Frequency	σ_2/σ_1	d (Meters)	5 WPM		20 WPM		80 WPM		320 WPM	
			KM	Miles	KM	Miles	KM	Miles	KM	Miles
100 cps	$\sigma_2/\sigma_1 = 1$		4.3	2.7	3.45	2.1	2.72	1.7		
	$\sigma_2/\sigma_1 = 0.1$	10	9.3	5.8	7.4	4.6	5.85	3.6		
		100	9	5.6	7.2	4.5	5.6	3.5		
		1000	5.9	3.7	4.4	2.7	3.3	2.1		
	$\sigma_2/\sigma_1 = 0.01$	10	20	12.4	15.6	9.7	12.4	7.7		
		100	16	10	12	7.5	9	5.6		
		1000	6.2	3.9	4.5	2.8	3.3	2.1		
1 kc			4.1	2.6	3.3	2.1	2.6	1.6	2.1	1.3
3 kc			6	3.7	4.8	3.0	3.8	2.4	3	1.9
10 kc			1.9	1.2	1.53	0.95	1.2	0.75	0.98	0.61
30 kc			5.0	3.1	2.5	1.6	1.47	0.91	1.16	0.72
100 kc			50	31	25	16	12.6	7.8	6.4	4.0

50X1

(a) Bandwidth = 1 CPS (5 WPM)

(b) Bandwidth = 4 CPS (20 WPM)

(c) Bandwidth = 16 CPS (80 WPM)

(d) Bandwidth = 64 CPS (320 WPM)

Page 29
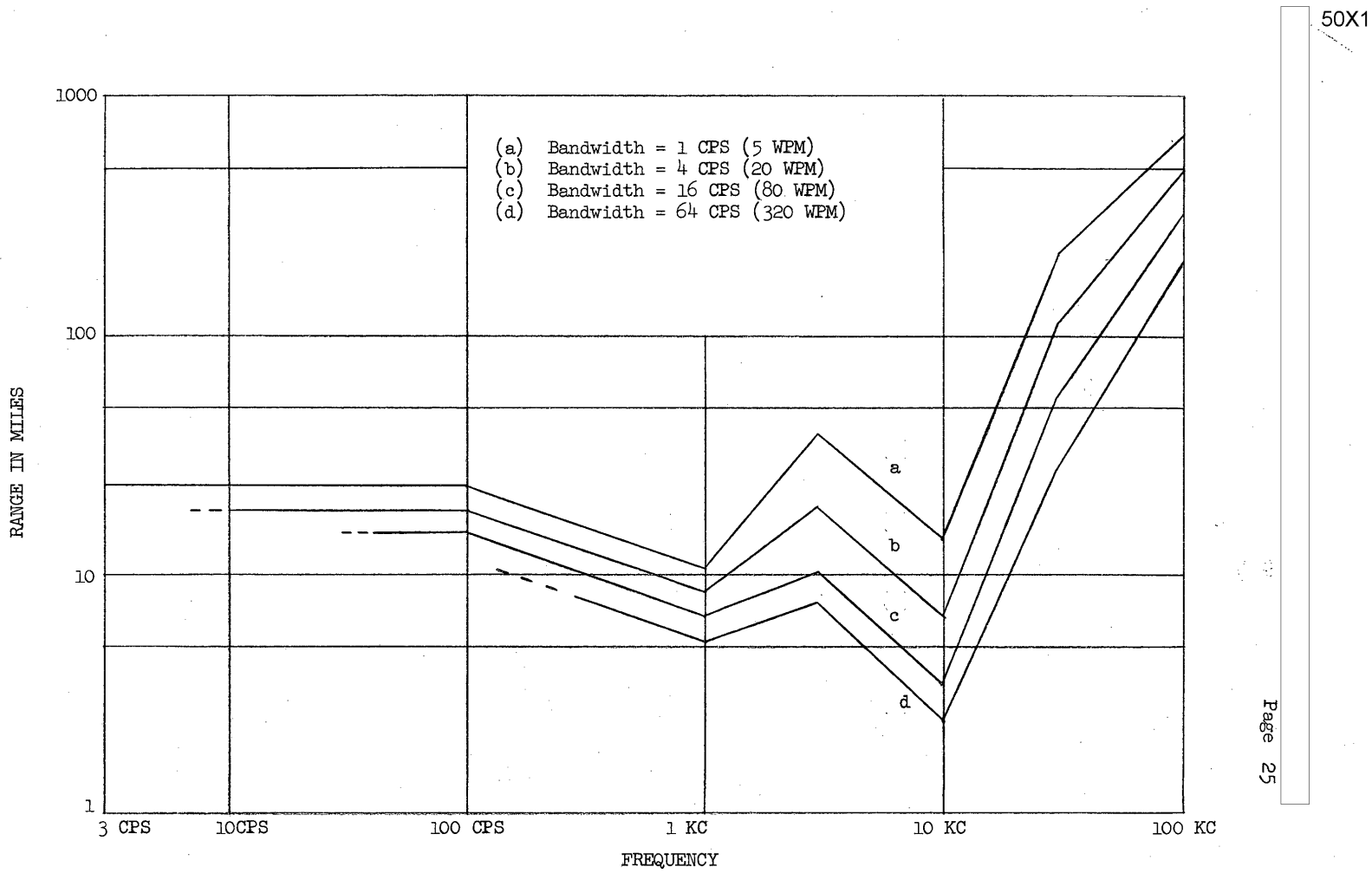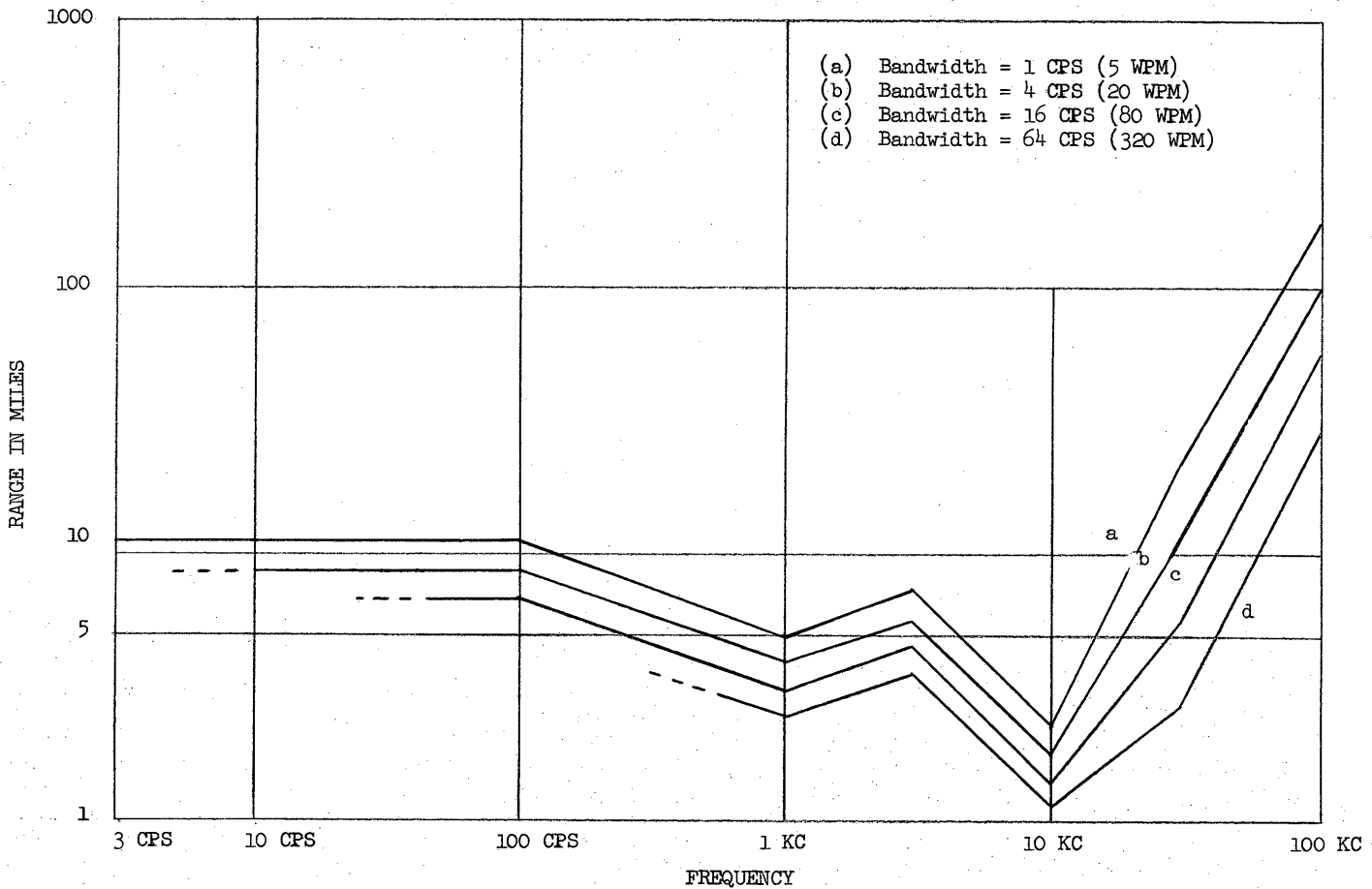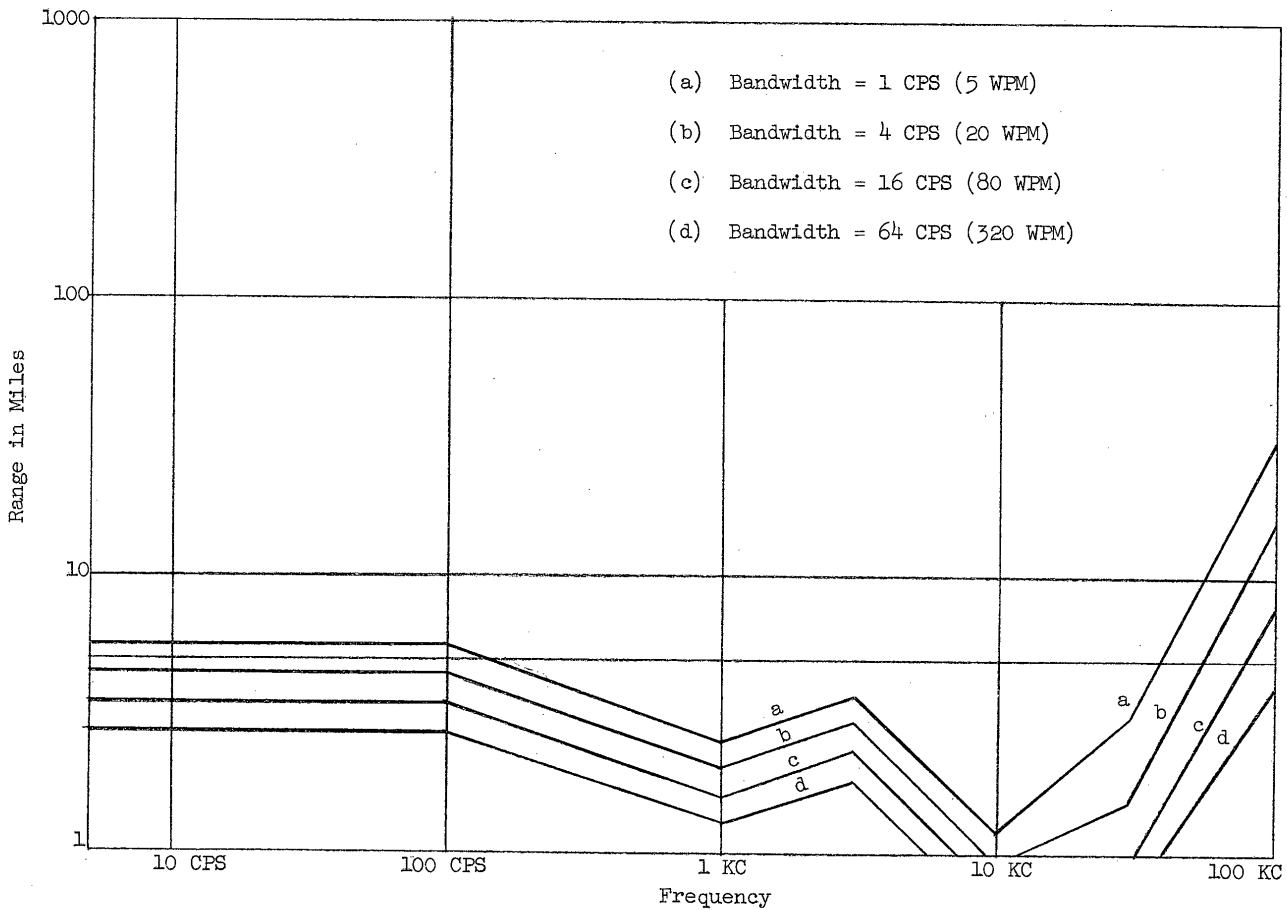
FIGURE 16. Communication Range vs. Frequency and Data Rate
(Low Noise, 1 Watt, $\sigma_2/\sigma_1 = 0.1$, d = 100 Meters)

50X1

TABLE IV

COMMUNICATION RANGE VS. FREQUENCY AND DATA RATE

HIGH NOISE, 1 WATT POWER

Frequency	σ_2/σ_1	d (Meters)	5 WPM		20 WPM		80 WPM		320 WPM	
			KM	Miles	KM	Miles	KM	Miles	KM	Miles
100 cps	$\sigma_2/\sigma_1 = 1$		1.97	1.22	1.56	0.97	1.25	0.78		
	$\sigma_2/\sigma_1 = 0.1$	10	4.3	2.7	3.44	2.14	2.72	1.7		
		100	4	2.5	3.13	1.95	2.4	1.5		
		1000	2.28	1.42	1.70	1.05	1.3	0.8		
	$\sigma_2/\sigma_1 = 0.01$	10	9.1	5.65	7.3	4.5	5.6	3.5		
		100	6	3.7	4.4	2.7	3.1	1.92		
		1000	2.28	1.42	1.70	1.05	1.3	0.8		
1 kc			1.9	1.2	1.54	0.95	1.2	0.75	0.98	0.61
3 kc			2.8	1.7	2.2	1.4	1.8	1.1	1.42	0.88
10 kc			0.90	0.56						
30 kc			1.1	0.68	0.90	0.56	0.70	0.44		
100 kc			5.0	3.1	2.6	1.6	1.26	0.78		

50X1

(a) Bandwidth = 1 CPS (5 WPM)
(b) Bandwidth = 4 CPS (20 WPM)
(c) Bandwidth = 16 CPS (80 WPM)
(d) Bandwidth = 64 CPS (320 WPM)

RANGE IN MILES

1000

100

10

1

10 CPS   100 CPS   1 KC   10 KC   100 KC
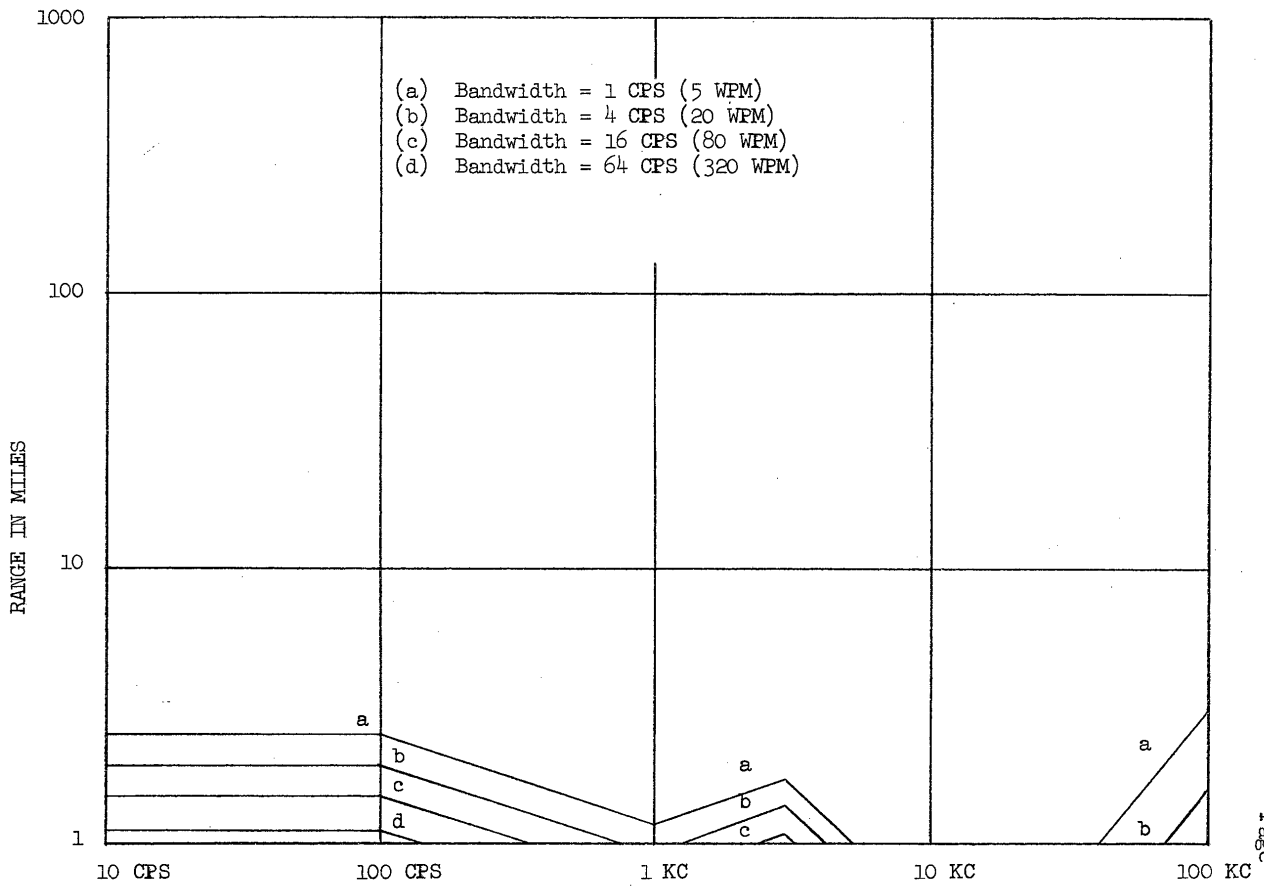
Page 31

FIGURE 17. Communication Range vs Frequency and Data Rate

(High Noise, 1 Watt, σ_2/σ_1 = 0.1, d = 100 Meters)

2.6   EQUIPMENT SIZE AND WEIGHT

The necessary equipment for a portable station in general consists of:
(1) electronic equipment and its carrying cases (including batteries, if any);
(2) wire to connect to electrodes (100 meters of wire required); and (3) elec-
trodes (stakes) and a hammer or other means of driving and extracting them. The
electrodes may consist of ordinary iron pipe driven about 3 to 5 feet into the
ground, or they may consist of existing buried conductors (water pipes, iron sur-
vey stakes, etc.). The wire need only be large enough so that its resistance be
not more than a few ohms. For example, wire as small as AWG No. 18 copper wire
can be used. A 100 meter length of this wire weighs a little over one pound and
has a resistance of about two ohms. The heat dissipation in such a wire is about
200 watts for a 5000-watt transmitter, or less than one watt per lineal foot of
wire. Larger wire can be used at a slightly increased weight penalty. However,
in this report, further size and weight considerations will be limited to that of
the electronic equipment and its carrying cases.

A transmitter power of 5000 watts can be supplied by batteries. Power can
be supplied by silver-zinc cells, for a total battery weight of about 100 lbs. The
cells can be recharged from the power line by a rectifier weighing about 2 lbs. The
coder/decoder is estimated to weigh one pound with a transistorized receiver weight
of half a pound. The transmitter itself would be transistorized and would weigh in
the neighborhood of 20 lbs. Weight of carrying cases (2 or 3) is estimated at 26 1/2
lbs., giving a total weight of 150 lbs. The weight can be summarized as follows:

Batteries	100	lbs.
Transmitter	20	lbs.
Coder/decoder	1	lb.
Receiver	0.5	lb.
Rectifier	2	lbs.
Case	26.5	lbs.
TOTAL	150	lbs.

Batteries which will meet this minimal weight requirement have a relatively
short life. They will provide operation for a 15-minute period, and require about
3 hours to reach a full charge. They can be recharged 25 times. Greater battery

life and shorter recharge time can be obtained at an extra penalty in battery weight. This 5000-watt transmitter provides 10 amperes into a (50 ohm) 100 meter antenna terminated in driven pipe electrodes.

At the other end of the power spectrum, a one-watt transmitter can be considered. The battery for such a transmitter would be a rechargeable type capable of about 100 recharge cycles and would weigh 8 ounces. The total weight breakdown is as follows:

Battery	8 oz.
Transmitter	8 oz.
Coder/decoder	1 lb.
Receiver	8 oz.
Rectifier and case	8 oz.
TOTAL	3 lbs.

For an a-c line-powered transmitter, the weight of batteries is eliminated, but allowance must be made for power conversion equipment.

Figure 18 shows a summary of battery weight and total weight estimates for both battery-powered and a-c line-powered sets as a function of transmitter power. Figures 19 and 20 show range in miles vs. transmitter power for 5 wpm and 80 wpm data rates. Indicated on the power scale are several representative set sizes.

50X1

Page 34
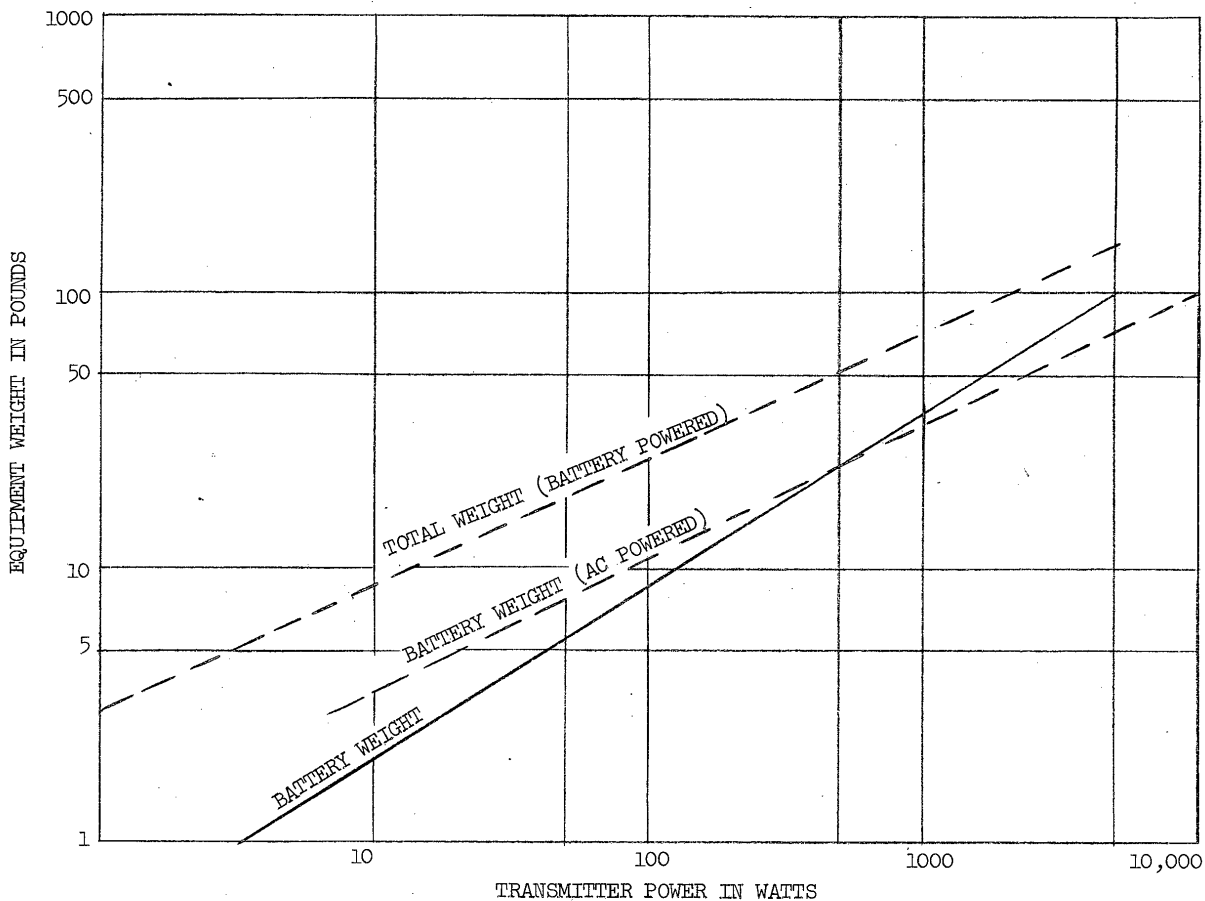
FIGURE 18. Equipment Weight vs. Transmitter Power

50X1

BATTERY POWERED "POCKET" SIZE 3 LBS.	BATTERY POWERED 10 LBS.	BATTERY POWERED 25 LBS	AC POWERED 25 LBS.	BATTERY POWERED 150 LBS

AC POWERED 100 LBS.

RANGE IN MILES vs **POWER IN WATTS**

f = 100 KC LOW NOISE

f = 30 KC LOW NOISE

f = 100 KC HIGH NOISE

f = 100 KC LOW NOISE

f = 3 KC LOW NOISE

f = 100 KC HIGH NOISE

f = 3 KC HIGH NOISE

f = 30 KC HIGH NOISE

Page 35
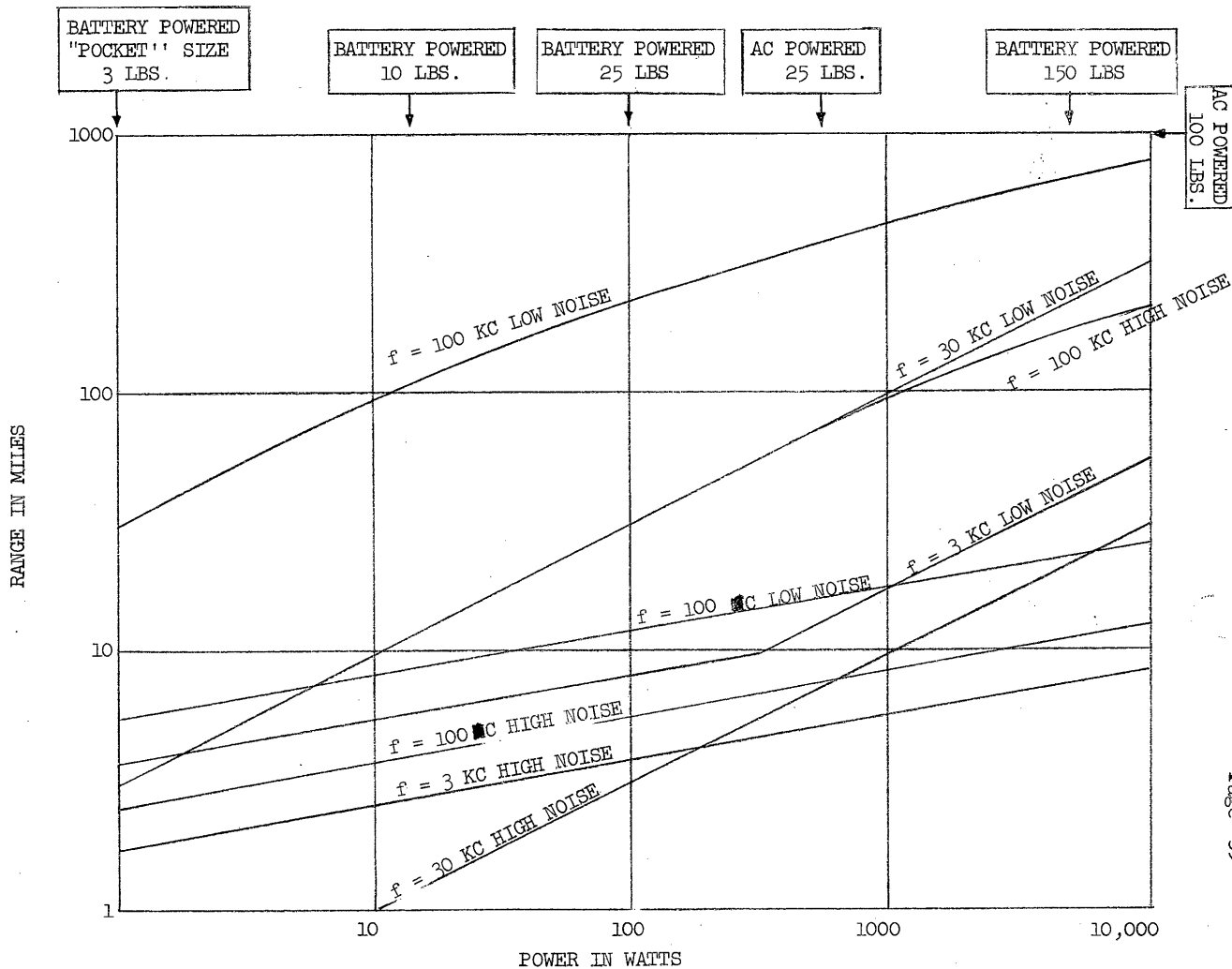
FIGURE 19. Range vs. Power For 5 WPM Data Rate

BATTERY POWERED "POCKET" SIZE 3 LBS.	BATTERY POWERED 10 LBS.	BATTERY POWERED 25 LBS.	AC POWERED 25 LBS.	BATTERY POWERED 150 LBS.	AC POW-ERED 100 LBS.

50X1

RANGE IN MILES vs **POWER IN WATTS**

f = 100 KC LOW NOISE

f = 30 KC LOW NOISE

f = 100 KC HIGH NOISE

80 WPM

f = 100 CPS LOW NOISE

f = 3 KC LOW NOISE

f = 100 CPS HIGH NOISE
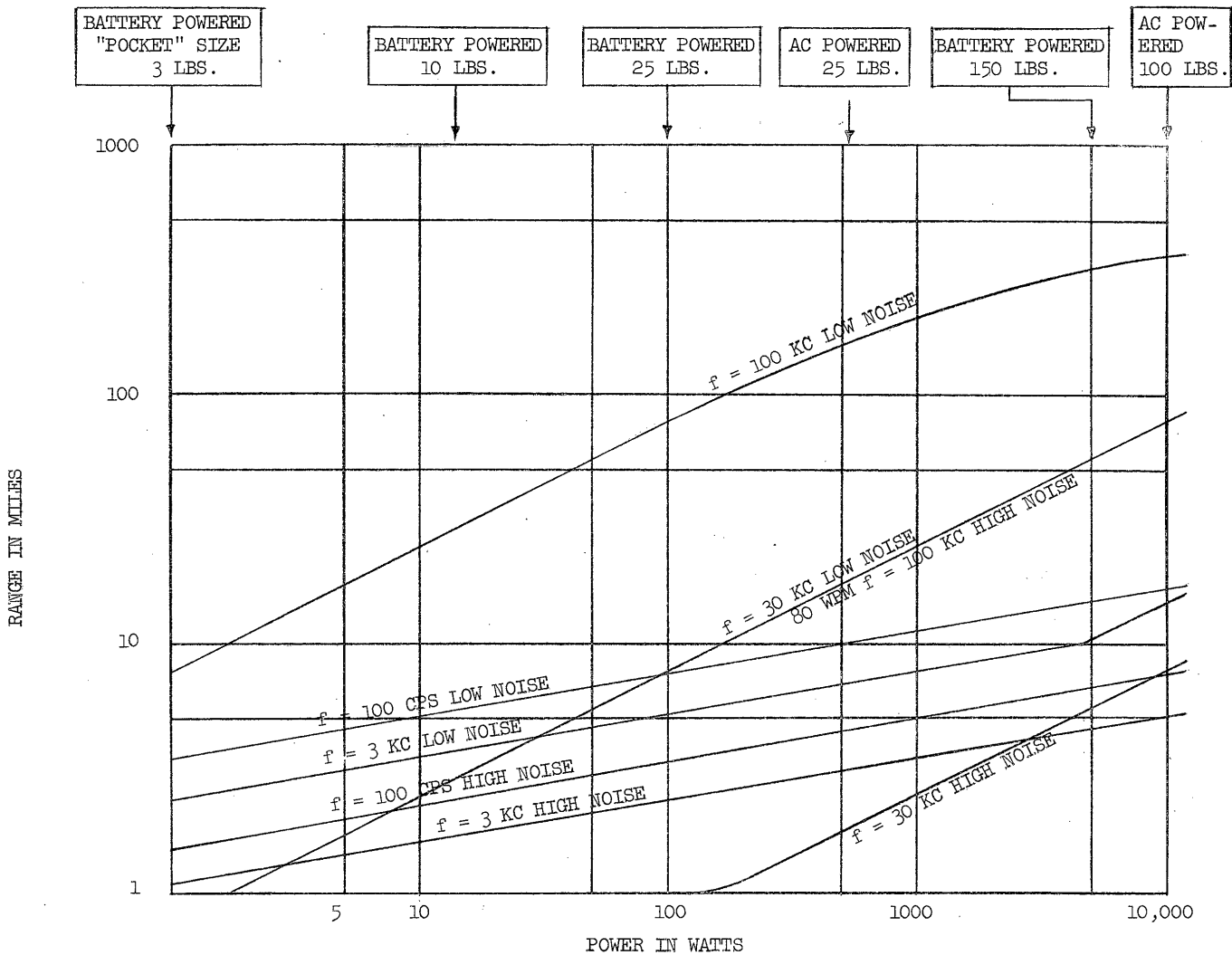
f = 3 KC HIGH NOISE

f = 30 KC HIGH NOISE

FIGURE 20. Range Vs Power For 80 WPM Data Rate

SECTION III

CONDUCTING LAYER PROPAGATION

3.1   INTRODUCTION

In the surface wave type of earth current propagation (cf. Section II), the transmitting and receiving antennas use electrodes at the surface of the earth, but the greater part of the actual propagation of usable energy takes place at the earth air interface in the form of a surface wave. It is also possible to conceive of a system in which the chief propagation path is through the earth itself. Such a system can ordinarily be expected to suffer much greater signal attenuation. By use of appropriate receiving electrode configurations, however, the noise may be greatly reduced in detecting such signals, and thus communication can be established at appreciable ranges.

In this study, a vertically spaced electrode configuration will be assumed for both transmitter and receiver. This configuration is less efficient for launching a surface wave, but more efficient for launching an earth-propagated wave. The lower electrode may be placed at the bottom of a water well or other vertical shaft in the earth. An upper electrode (e.g., a driven iron rod) is required at the surface. An artist's conception of such a communication system is shown in Figure 21.

3.2   NOISE CHARACTERISTICS FOR VERTICAL ELECTRODE CONFIGURATION

The noise voltage appearing between the electrodes arises from atmospheric distrubances, telluric currents and magnetic disturbances. Above approximately one cycle per second, the chief source of noise is atmospheric in origin. Telluric and magnetic micropulsations have some effect at these frequencies, but some preliminary measurements of the vertical component of potential at extremely low frequencies in drilled wells have given values on the order of 40 db less than the horizontal. Field measurements of vertical underground noise have, however, not been as extensive as those at and above the surface of the earth. Thus the characteristics of the noise must be reduced from the characteristics of the atmospheric noise at the surface. Since the surface noise arises chiefly from vertically polarized surface waves in the atmosphere, this source will be assumed in the subsequent analysis.

In the propagation of a surface wave over an imperfect conductor such as the earth, a set of inhomogeneous plane waves is generated within the conductor. In the case of the earth, and at the frequencies of interest here, the electric field
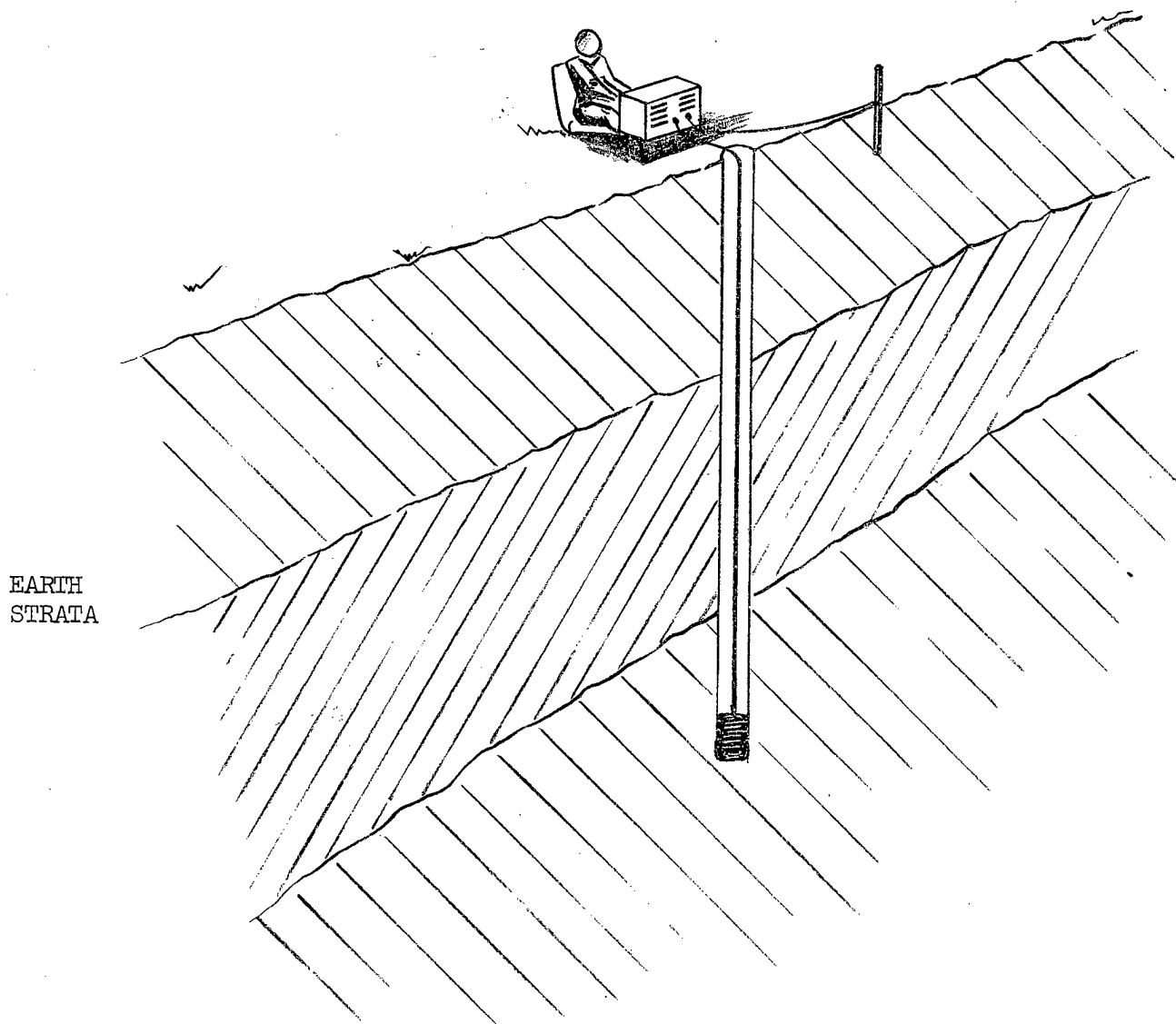
50X1

Page 39

EARTH
STRATA

FIGURE 21.   Vertical Electrode Configuration

in the earth is much smaller than that in the air, and the earth waves propagate almost vertically downward. The planes of constant phase are not exactly parallel to the planes of constant amplitude. The vertical component of electric field $E_V(Z)$ varies with depth z according to the relation

$$E_V(z) = E_V(o) \, \mathcal{E}^{-a(1-i)z}$$

where

$$a = \sqrt{\frac{\omega \mu_o \sigma}{2}} .$$

The ratio of the horizontal field to the vertical field within the earth at the surface is given by

$$\frac{E_H(o)}{E_V(o)} = \sqrt{\frac{\sigma}{\omega \mathcal{E}_o}} .$$

Thus

$$E_V(z) = \sqrt{\frac{\omega \mathcal{E}_o}{\sigma}} \; E_H(o) \, \mathcal{E}^{-a(1-i)z}$$

where $E_H(o)$ is the horizontal field at the surface. Since $\sqrt{\dfrac{\omega \mathcal{E}_o}{\sigma}}$ is much less than unity, the vertical field is much smaller than the horizontal. To find the potential difference between vertically spaced electrodes, it is only necessary to integrate $E_V(z)$. Thus

$$V_D = \int_o^D E_V(z) \, dz$$

$$= \sqrt{\frac{\omega \mathcal{E}_o}{\sigma}} \; E_H(o) \int_o^D \mathcal{E}^{-a(1-i)z} \, dz$$

from which

$$\left| V_D \right| = \frac{1}{\sqrt{2} \, a} \cdot \sqrt{\frac{\omega \mathcal{E}_o}{\sigma}} \; E_H(o) \left| \mathcal{E}^{-aD} \, \mathcal{E}^{iaD} - 1 \right|$$

A plot of $\dfrac{V_D}{E_H\,(o)}$ is given in Figure 22 for lower electrode depths of 10, 30, 100, and 300 meters for $\sigma = 10^{-2}$ mho/meter. Using the low and high noise values for $E_H\,(o)$ as shown in the section on surface wave propagation gives the final noise voltages as plotted in Figures 23 and 24.

3.3 PROPAGATION OF EARTH CURRENTS FROM VERTICALLY SPACED ELECTRODES

It is assumed that one electrode is located at the surface, and the other at depth d in the earth.

3.3.1 Homegenous Earth

The analysis is relatively simple in the static case for a homogeneous earth. The situation may be diagrammed as shown in Figure 25. It is assumed that the upper electrode (No. 1) carries current +I and the lower electrode (No. 2) carries -I. Then the voltage V_v measured by a receiver at range r is the difference in potential between electrodes Nos. 3 and 4. Using the method of images, this potential difference is found to be

$$V_v = \frac{3I}{4\pi\,\sigma\,r} - \frac{I}{\pi\sigma\,r\sqrt{1 + (\frac{d}{r})^2}} + \frac{I}{4\pi\,\sigma\,r\sqrt{1 + 4(\frac{d}{r})^2}}$$

which reduces to

$$V_v \cong \frac{9\,I\,d^4}{8\pi\,\sigma\,r^5} \;,\; \text{neglecting higher order terms.}$$

If a horizontal electrode spacing d were used at the surface of the earth, the potential difference between electrodes would be

$$V_H = \frac{3\,I\,d^3}{4\pi\,\sigma\,r^4}$$

This is greater than V_v at all ranges of interest, and thus it might appear better to use a horizontal antenna for receiving. However, the noise is much less for the vertical electrode spacing. For example, if a 100-meter electrode spacing is used, the noise for a vertical configuration at a frequency of 100 cps is -23.5 db relative to 1μv for a horizontal field of 1μv/m, as can be seen from Figure 22.
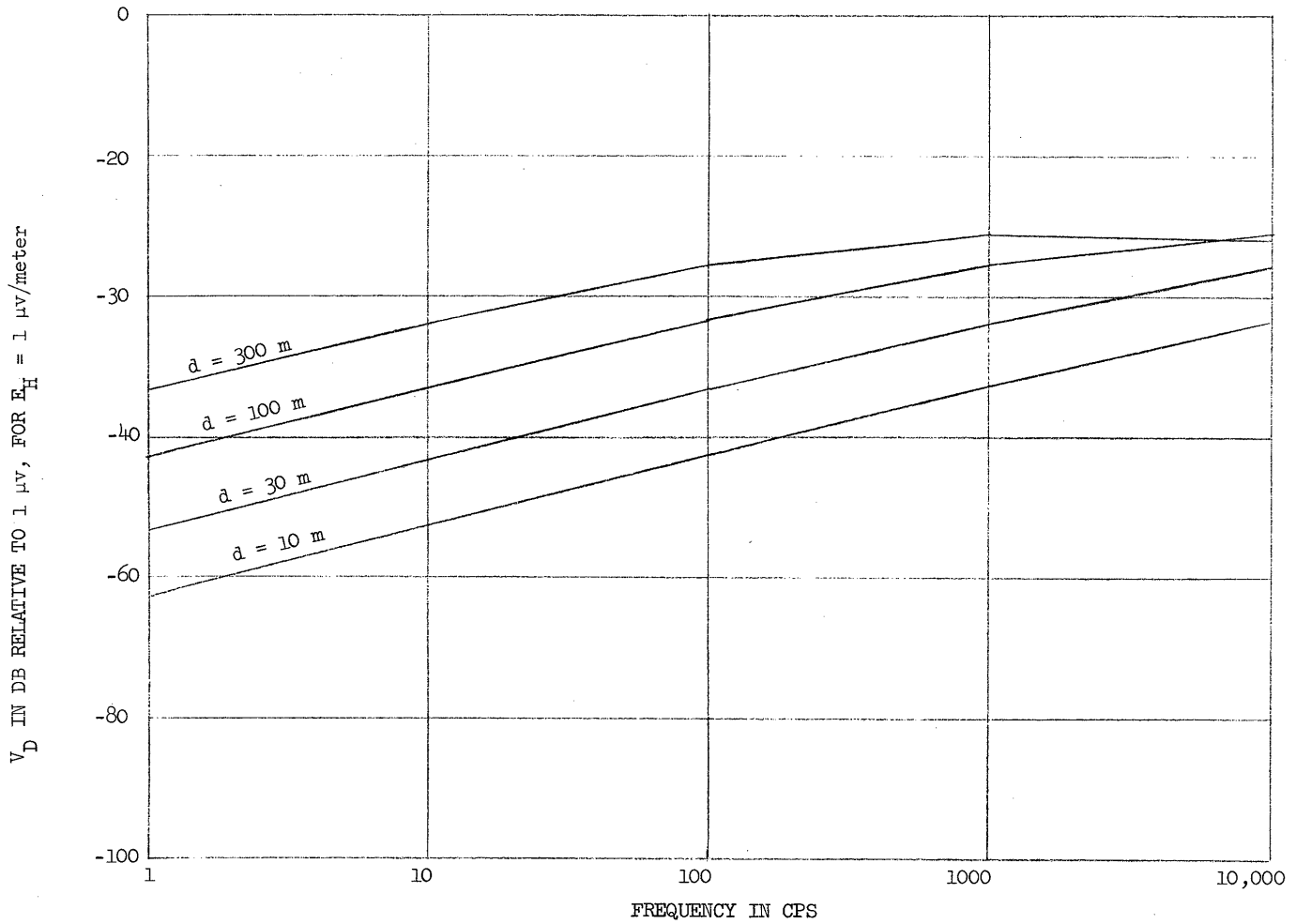
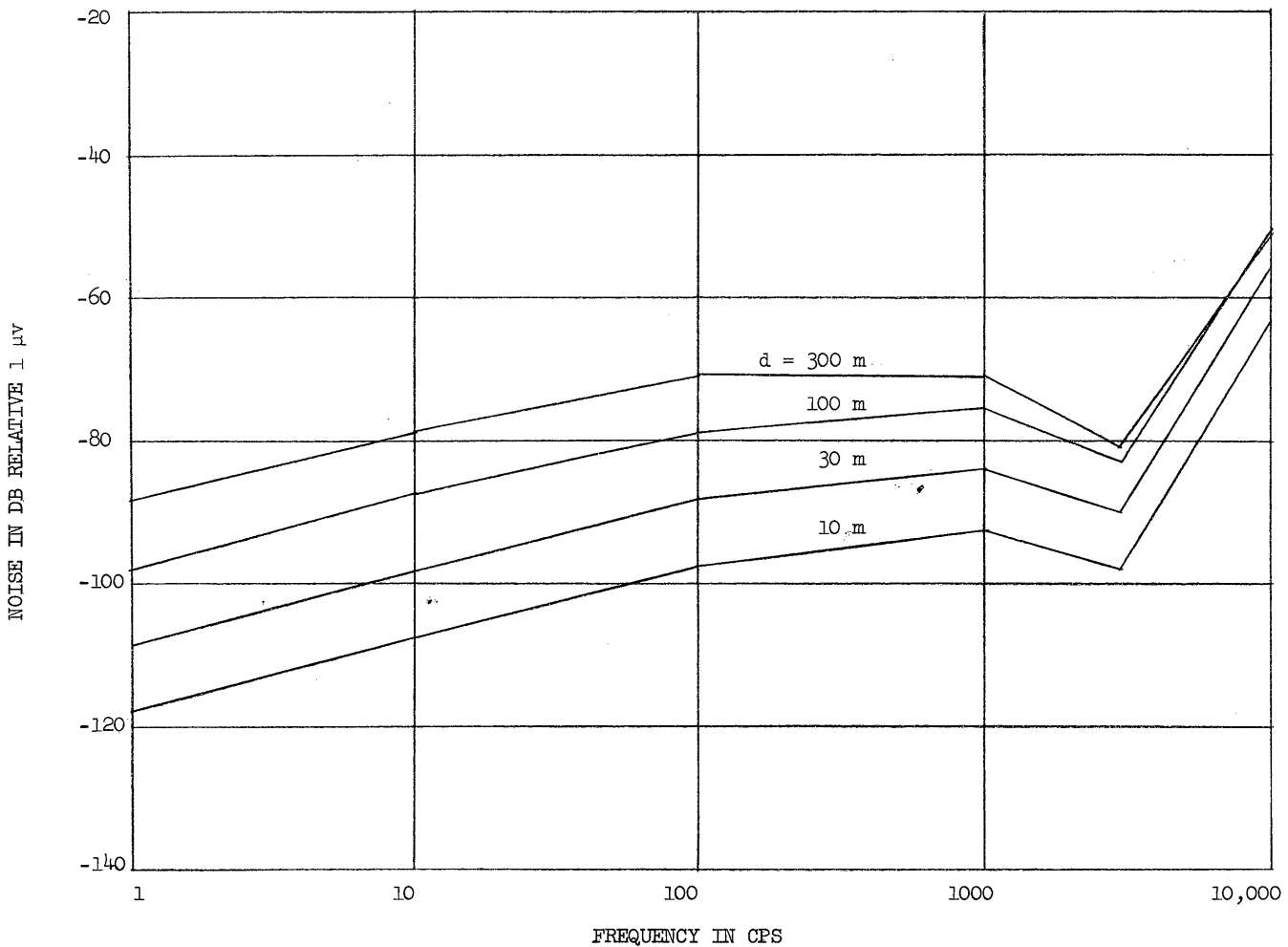FIGURE 22. Ratio of Vertical Received Noise to Horizontal
Noise At Surface

50X1

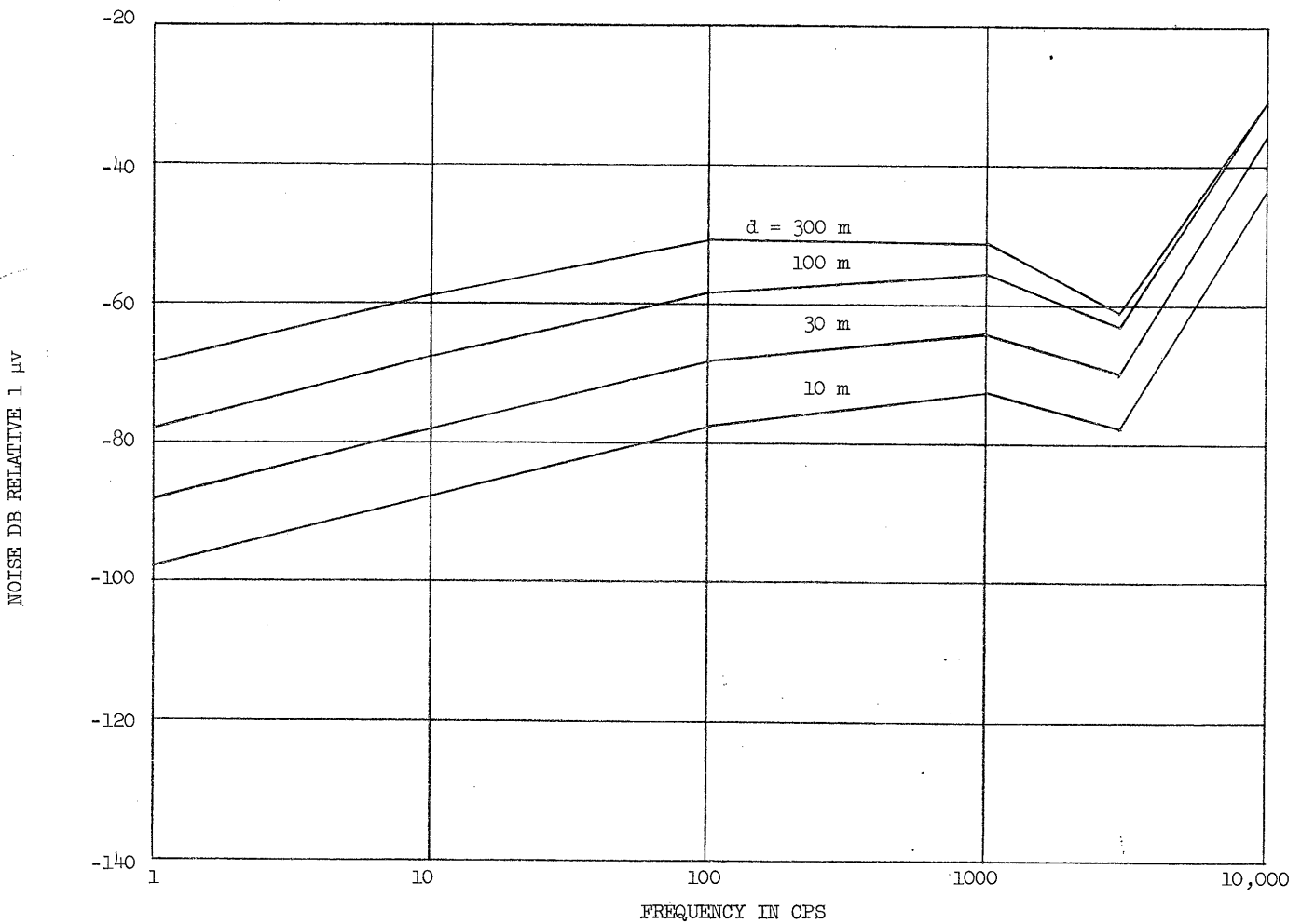FIGURE 23.   Received Noise vs. Frequency (One Cycle Bandwidth)

50X1

FIGURE 24. Received Noise vs. Frequency (One Cycle Bandwidth)

r

TRANSMITTER   RECEIVER
    ELECTRODE NO. 1 V_v

                    NO. 3
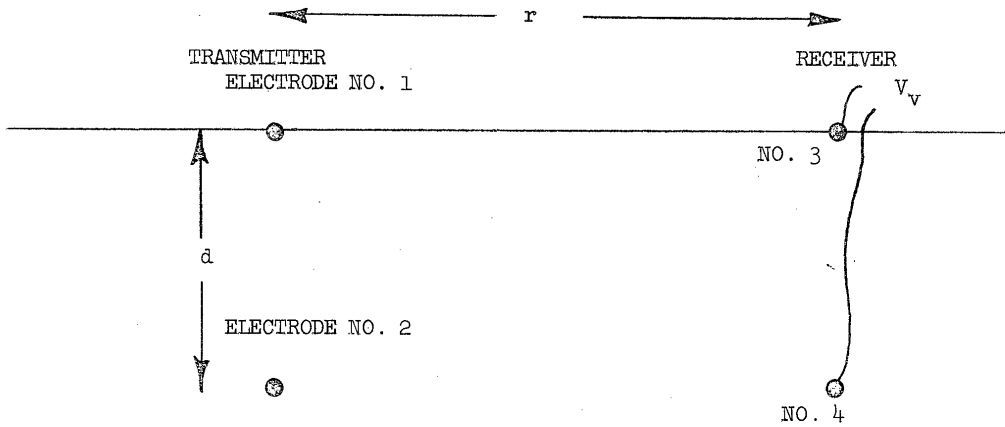
d

    ELECTRODE NO. 2

                    NO. 4

FIGURE 25.   Homogeneous Earth

The corresponding noise in a 100 meter horizontal antenna would be +40 db relative to 1μv. Thus the ratio of horizontal to vertical noise is 63.5 db at 100 cycles/second. This result applies to spacings up to about 1000 meters. At greater spacings, the ratio is still larger. At 10 kc, the ratio is about 50 db for spacings of 100 meters or less, and greater for greater spacings. Taking the applicable ratio to be 60 db means that it is advantageous to use the vertical electrode configuration provided that

$$\frac{V_H}{V_V} = \frac{2}{3}\frac{r}{d} = 1000$$

This implies that, for d = 100 meters,

$$r \leqslant 150 \text{ kilometers, or}$$
$$r \leqslant 93 \text{ miles}$$

Thus, at ranges less than about 93 miles, the vertical electrode spacing is preferable.

It is worth noting that in the case where the transmitter uses horizontally spaced electrodes at the surface, the ratio is

$$\frac{V_H}{V_V} = \frac{2 r}{d}$$

which would imply that vertical receiving electrodes are advantageous at ranges less than about 30miles. However, horizontal transmitting electrodes are more efficient at launching a surface wave in the air, which carries most of the received energy. In such a case the ratio of $\frac{V_H}{V_V}$ is the same as for the noise, since both arrive as surface waves.

3.3.2 Layered Earth

When certain layering conditions occur in the surface region of the earth's crust, the received signal may be enhanced over that for a homogeneous earth. For example, suppose that there is a surface layer of high conductivity, underlain by a layer of low conductivity, followed by another layer of high conductivity, and all underlain by a basement of low conductivity. This situation is diagrammed in Figure 26. If electrodes are placed as shown in the figure, then
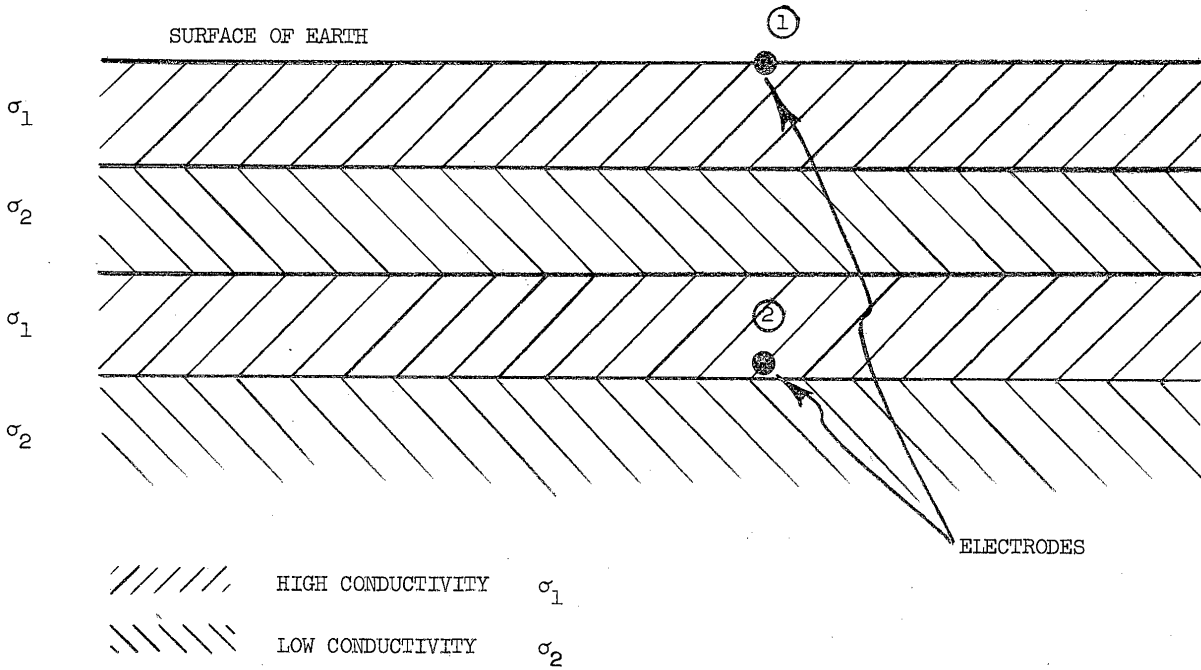
50X1

SURFACE OF EARTH

σ_1

σ_2

σ_1

σ_2

ELECTRODES

///// HIGH CONDUCTIVITY σ_1

\\\\\ LOW CONDUCTIVITY σ_2

FIGURE 26. Layered Earth

Page 47

the two conducting layers, separated by the relatively non-conducting layer, act to increase the signal received between similarly spaced receiving electrodes. The structure acts crudely like a lossy flat-plate waveguide, concentrating the propagation of energy between the layers to some extent. The degree of signal enhancement will depend on the conductivities and upon the relative thicknesses of the layers. For the purposes of this analysis, it will be assumed that a signal enchancement of 20 db is realized from a ratio of conductivities, $\sigma_2/\sigma_1 = 0.1$. The resulting curves of received potential difference vs. range are shown in Figure 27 for several values of electrode separation distance d.

3.3.3 Range, Frequency, and Data Rate Considerations

Range and data rate will be determined in a manner similar to that used in the previous section on surface waves. Thus a 5 wpm data rate requires a one cycle/second bandwidth and about 10 db signal-to-noise ratio.

An electrode impedance of 50 ohms will be assumed, as before, so that 5000 watts corresponds to 10 amperes electrode current. Figures 28 and 29 are plots of range vs. frequency under high and low noise for a 5000 watt transmitter for data rates of 5, 20, 80, and 320 wpm. Figures 30 and 31 are plots of range vs. power for a 5 wpm data rate, under the low and high noise conditions. Figures 32 and 33 are similar plots for an 80 wpm data rate.

3.3.4 Discussion

The vertically-spaced electrode method is in general well suited for short range communications, and has several unique advantages.

The electric field falls off very rapidly with distance (i.e., as range to the fifth power). This makes such a communication link virtually impossible for an enemy to jam from a distance, using similar equipment. An enemy could attempt to launch a jamming wave using horizontally spaced electrodes, but could do so with reasonable power only if his distance from the receiver were comparable to that of the communicating transmitter. Detection of the signal by an enemy will be extremely difficult because of the narrow bandwidths, low S/N ratio, the low frequencies used, and the rapid attenuation with distance. Conventional receivers and direction finders would be relatively ineffective.

This method is most applicable at the extremely low frequencies (below about 1 kc). The analysis given here covered only the static case. At frequencies
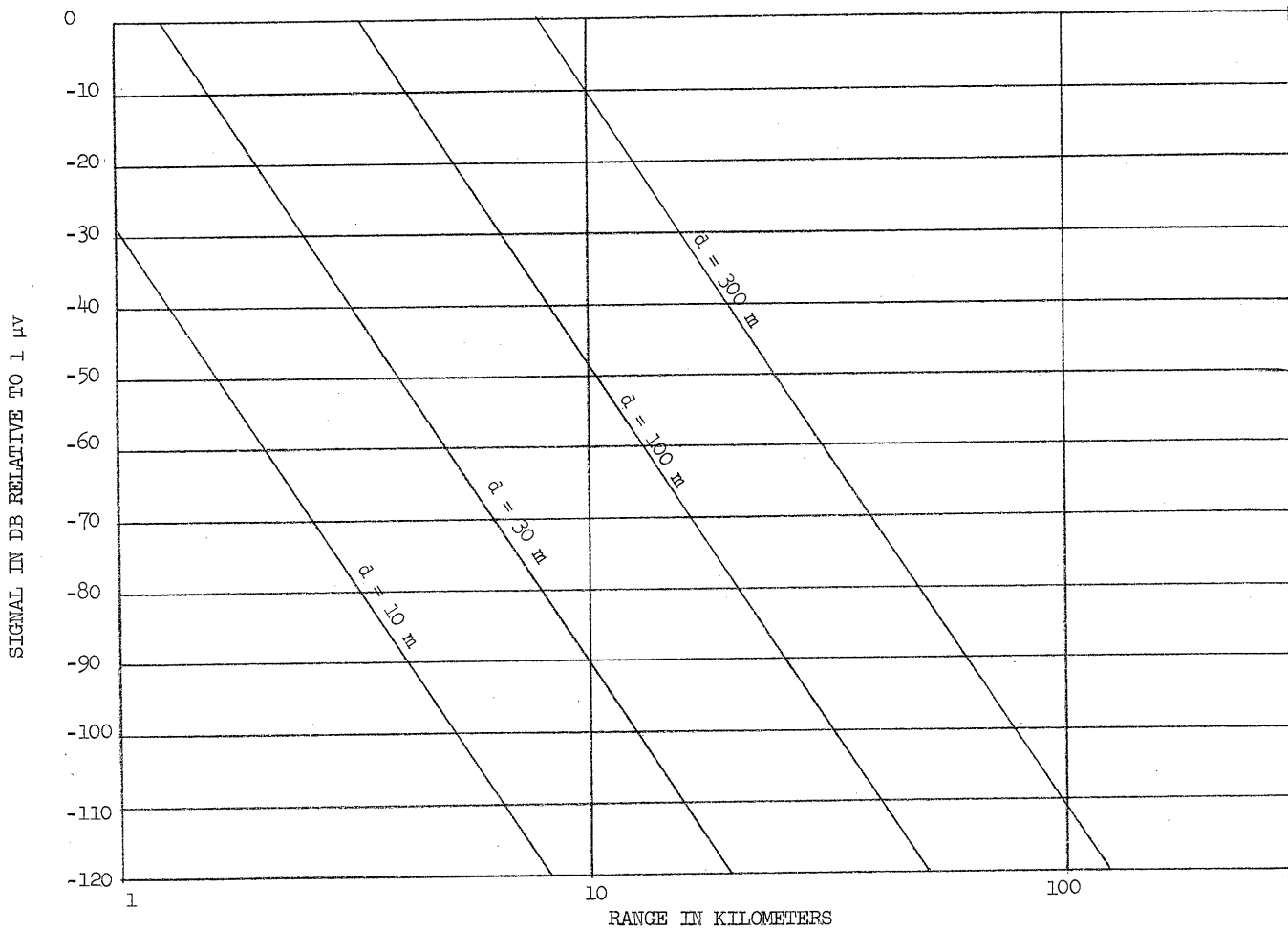
50X1

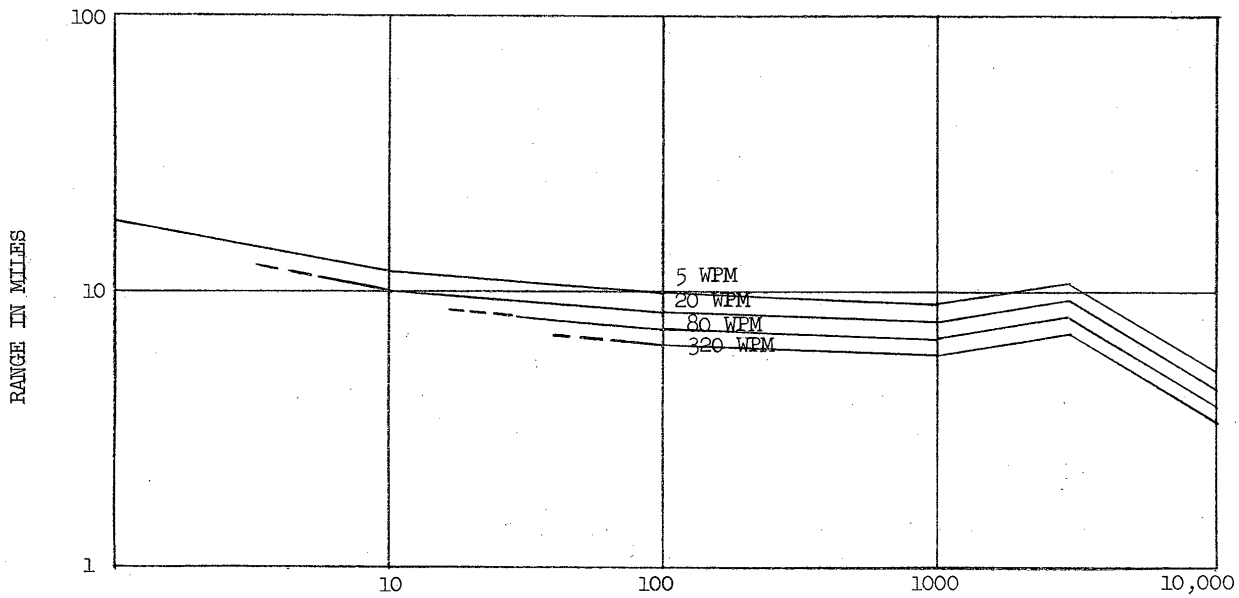FIGURE 27. Received Signal vs Range

I = 10 Amps

50X1

RANGE IN MILES

100

10

1

| | 10 | 100 | 1000 | 10,000 |

5 WPM
20 WPM
80 WPM
320 WPM

FIGURE 28.   Range vs. Frequency   Low Noise Condition

I = 10 AMPS
d = 100 METERS

Page 50

50X1
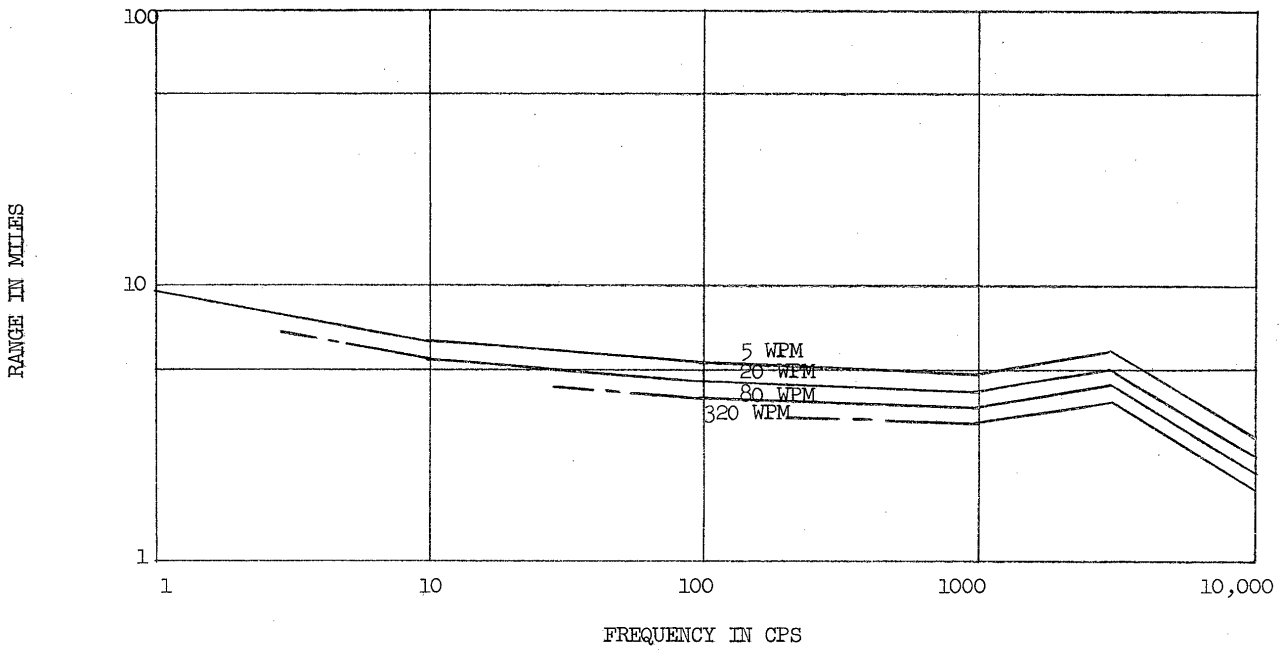
FIGURE 29.   Range Vs. Frequency   High Noise Condition

$$I = 10 \text{ AMPS}$$
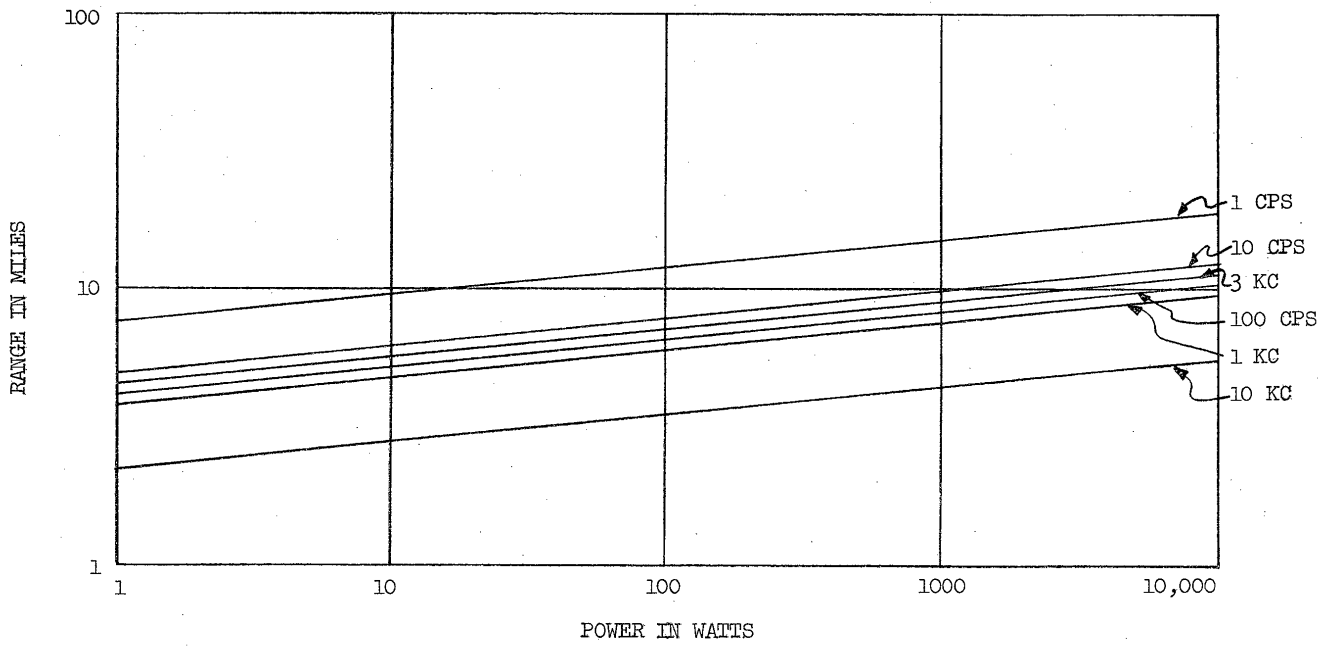$$d = 100 \text{ METERS}$$

50X1

FIGURE 30. Range vs. Power For 5 WPM Data Rate

Low Noise Condition

50X1
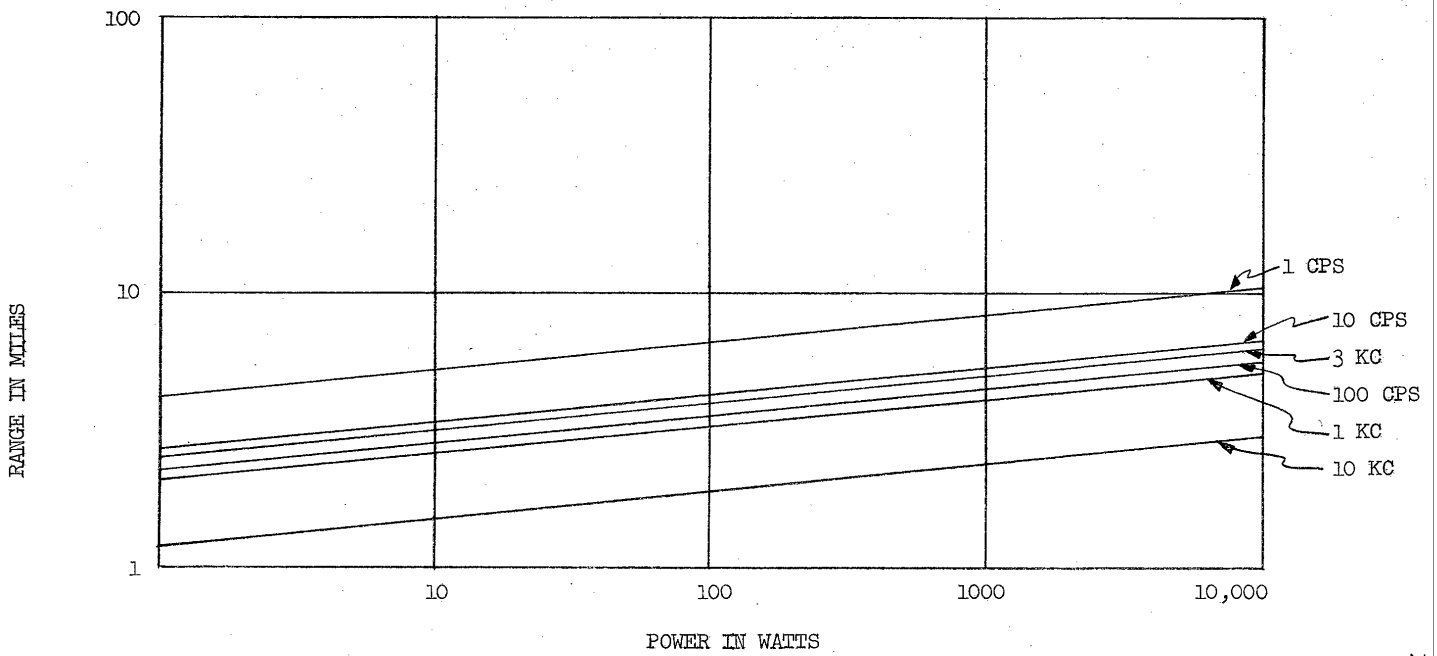

FIGURE 31. Range Vs. Power For 5 WPM Data Rate

High Noise Condition
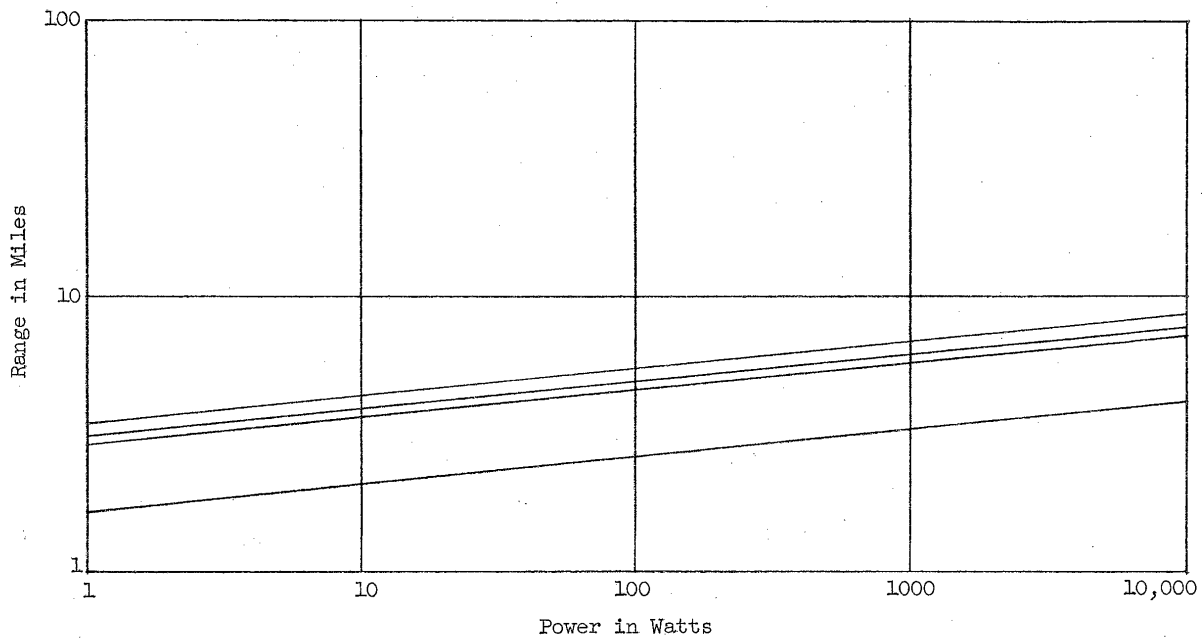
50X1

FIGURE 32. Range vs. Power for 80 WPM Data Rate(Low Noise Condition)
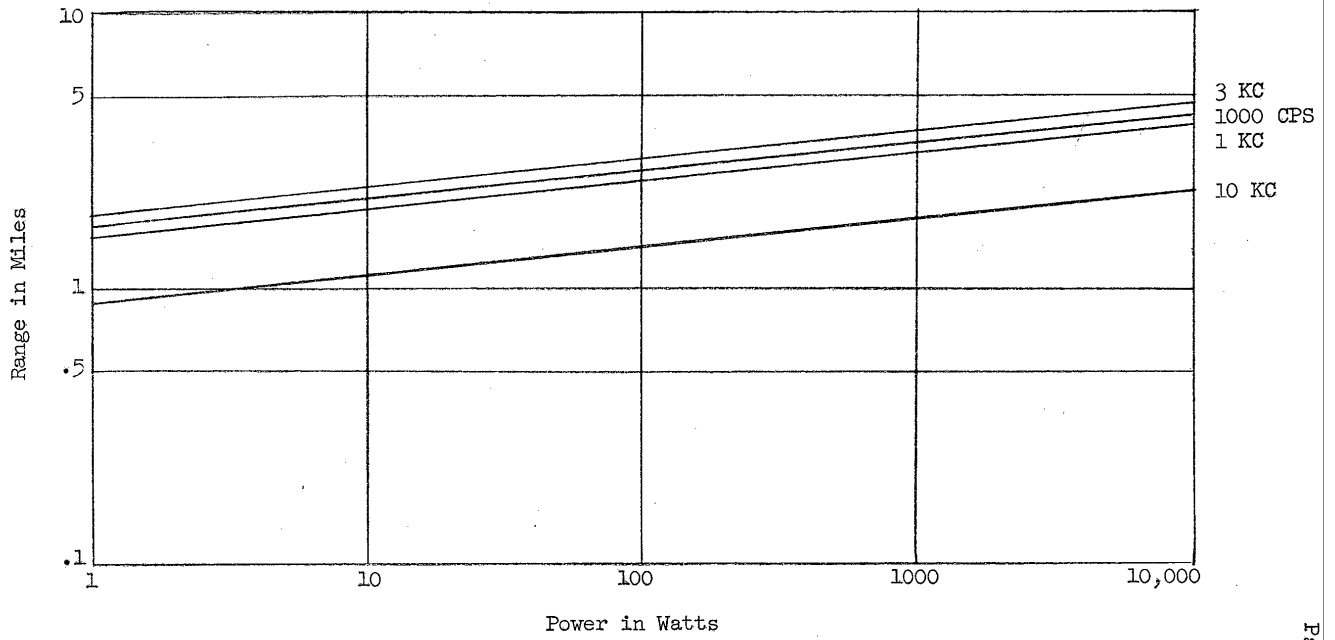
Page 54

50X1

FIGURE 33.   Range vs. Power for 80 WPM Data Rate (High Noise Condition)

Page 55

much above 1 kc, the attenuation of the earth begins to reduce the received signal strength still further. While some surface wave may be generated, the amplitude of such a wave would be far less than if horizontal electrodes were used.

While it is necessary to drill a "well" for the installation of the lower electrode, the installation when complete is quite inconspicuous (much less so than in the horizontal electrode case where a 100-meter wire must be strung along the surface of the earth). Also, all exposed parts of the installation are in a single location, so that accidental damage to the electrode cable is not a problem.

Portable equipment can be used for field stations, provided only that lower electrode installations be available wherever the stations are required to operate.

APPENDIX A

ULTRA LOW FREQUENCY EARTH CURRENT PROPAGATION

ULTRA-LOW FREQUENCY EARTH CURRENT PROPAGATION

I. Introduction

For propagation at short ranges, less than twice the height of the iono-
sphere, the effect of the curvature of the earth or the ionosphere should be
negligible. Theoretical assumptions and subsequent empirical testing has de-
monstrated that propagation may be analyzed on the basis of a flat earth and
no ionosphere. In the sub-paragraphs below, a theoretical treatment of the
direct current case, which is a useful approximation to propagation in the
ultra-low frequency range, will be given. In this treatment, a single layer
earth is assumed in which a surface layer overlies a base material of rela-
tively low conductivity. This is a useful approximation of the usual geo-
physical conditions of the earth in which the conductivity decreases with age
of the geological formation.

In higher frequency earth current propagation, it is unnecessary to
consider the conductivities at depths much greater than that at which the elec-
trodes are buried. This is true because the earth attenuation is higher at the
higher frequencies and the chief path of importance is upward from the electrodes
to the surface of the earth. For this case the radial component of the field,
in a direction along the axis of the earth current dipole, is:

$$E_\rho = \frac{IL}{2\pi\sigma\rho^3}\left\{1 - \left[\left(\frac{2\pi\rho^2}{\lambda}\right) + j\left(\frac{2\pi\rho}{\lambda}\right)\right]\epsilon^{-\left(d_t + d_r\right)\sqrt{\omega\mu\sigma/2}}\right\}$$

(Eq. 1)

where

|		
L	=	length of the horizontal element in meters
σ	=	ground conductivity in mhos per meter
λ	=	free space wavelength in meters
ρ	=	radial distance in meters
d_t	=	burial depth of transmitter in meters
d_r	=	burial depth of receiver in meters
μ	=	permeability of free space in MKS units
I	=	current in amperes

50X1

This equation has been verified at very low frequencies in many field tests
conducted by ⬚⬚⬚⬚⬚⬚ For ultra-low frequencies, where
distances are small compared to a wavelength, this equation indicates an
inverse range-cubed relationship.

The presence of a deeper layer of low conductivity appreciably alters the
range dependence factor when the frequency is low enough so that the lower layer
is on the order of a skin depth or less beneath the earth current electrodes.
As shown here for the DC current case, the range dependence factor is inverse
cubed at extremely short ranges and at extremely long ranges, but there is an
intermediate area in which the dependence is inverse range squared (smaller
attenuation versus distance). The presence of the lower layer results in a
long range signal advantage approximately equal to the ratio of conductivities.
The propagation characteristics result in integral equations which are not
expressable in closed form, but have been numerically integrated to obtain the
normalized curves shown here. It should be noted that although the analysis
considers the electrodes to be located at the surface, the surface potential for
ranges greater than one layer of depth would be very close to that shown even
for relatively deep burial of the electrodes within the upper layer. Similarly,
burial of the receiving antenna would cause negligible change.

II. General Considerations

Consider a current (I) flowing between two surface electrodes whose
spacing is denoted as 'a'. The resulting surface electric vector can be con-
sidered to be composed of radial and angular components as shown in the sketch
below.
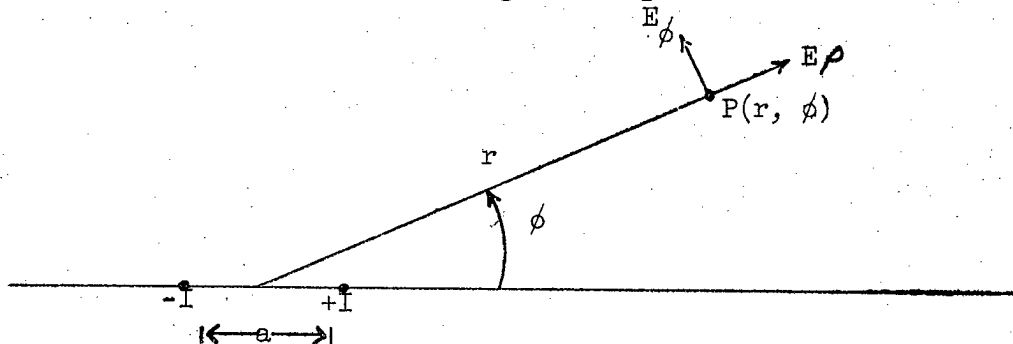
The potential at the point P is given by:

$$V_P(r, \phi) \cong V\left(r - \frac{a}{2} \cos \phi\right) - V\left(r + \frac{a}{2} \cos \phi\right)$$

$$\cong -a \cos \phi \frac{dV}{dr} \quad r \gg a \qquad \text{(Eq. 2)}$$

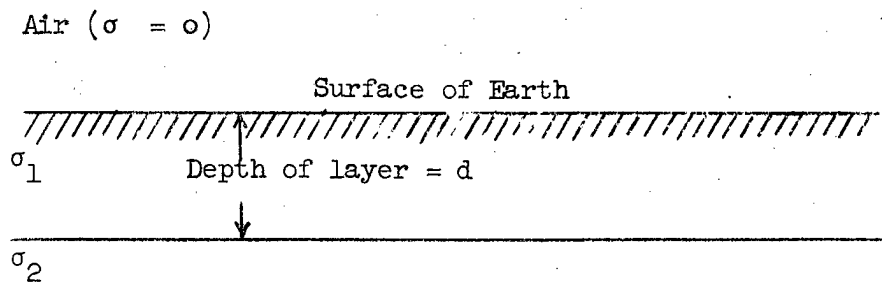where $V(r)$ is the potential at range r from a single current source of $+I$. Then:

$$E_\rho = \frac{\partial V_P(r, \phi)}{\partial r} \cong -a \cos \phi \frac{d^2 V}{dr^2} \qquad \text{(Eq. 3)}$$

and

$$E_\phi = \frac{1}{r} \frac{\partial V_P(r, \phi)}{\partial \phi} \cong a \sin \phi \frac{dV}{dr} \cdot \frac{1}{r} \qquad \text{(Eq. 4)}$$

III. The Surface Potential from a Monopole

The earth model considered is diagrammed below:

Air ($\sigma = 0$)

Surface of Earth

//

σ_1 Depth of layer $= d$

σ_2

The surface potential due to a current monopole of strength $+I$ (i. e. an earth current electrode near the surface carrying current $+I$) can be found using the method of images to be:

$$V = \frac{I}{2\pi\sigma_1} \left[\frac{1}{r} + 2 \sum_{i=1}^{\infty} \frac{a^i}{\sqrt{r^2 + 4i^2 d^2}} \right] \qquad \text{(Eq. 5)}$$

where: $a = \dfrac{1 - \sigma_2/\sigma_1}{1 + \sigma_2/\sigma_1}$

At short ranges the potential approaches the asymptote

$$V \Big|_{r/d \to 0} \longrightarrow \frac{I}{2\pi\sigma_1 r} \qquad \text{(Eq. 6)}$$

This is the potential which would exist for all ranges on a homogeneous earth of conductivity σ_1.

At long ranges, the potential approaches the asymptote

$$V \Big|_{\substack{r/d \to \infty \\ \sigma_2 \neq 0}} \longrightarrow \frac{I}{2\pi\sigma_2 r} = \frac{1}{(\sigma_2/\sigma_1)} \cdot \frac{I}{2\pi\sigma_1 r} \qquad \text{(Eq. 7)}$$

In the singular case when $\sigma_2 = 0$, the radial rate of change of potential is asymptotic to:

$$\frac{dV}{dr} \Big|_{\substack{r/d \to \infty \\ \sigma_2 = 0}} \longrightarrow \frac{-I}{2\pi d\sigma_1 r} \qquad \text{(Eq. 8)}$$

The discrete image current distribution can be approximated by a continuous distribution and written, in one form, as:

$$V \cong \frac{I}{2\pi\sigma_1} \left\{ \frac{1}{r} + 2 \int_{1/2}^{\infty} \frac{e^x}{\sqrt{r^2 + 4d^2x^2}} \, dx \right\} \qquad \text{(Eq. 9)}$$

This approximation satisfies the asymptotic relations given above.

IV. **The Electric Vector from a Dipole**

(A) Radial Component

The radial component of the electric vector was given by Equation 3 as:

$$E_\rho \cong -a \cos \phi \, \frac{d^2 V}{dr^2}$$

By differentiating Equation 9, one obtains

$$\frac{dV}{dr} = \frac{-I}{2\pi\sigma_1} \left\{ \frac{1}{r^2} + 2r \cdot \int_{1/2}^{\infty} a^x \cdot \left(r^2 + 4d^2 x^2 \right)^{-3/2} dx \right\} \quad \text{(Eq. 10)}$$

and

$$\frac{d^2 V}{dr} \cong \frac{I}{\pi\sigma_1 d^3} \cdot \frac{1}{y^3} \cdot \left\{ 1 + \int_{1/2}^{\infty} \frac{\left[2 - \left(\frac{2x}{y} \right)^2 \right] a^x}{\left[1 + \left(\frac{2x}{y} \right)^2 \right]^{5/2}} \, dx \right\} \quad \text{(Eq. 11)}$$

where $y = r/d$

Thus, from Equation 3:

$$E_\rho \cong -\left[\frac{I \, a \cos \phi}{\pi\sigma_1 d^3} \right] \cdot \frac{1}{y^3} \cdot \left\{ 1 + \int_{1/2}^{\infty} \frac{\left[2 - \left(\frac{2x}{y} \right)^2 \right] a^x}{\left[1 + \left(\frac{2x}{y} \right)^2 \right]^{5/2}} \, dx \right\} \quad \text{(Eq. 12)}$$

A normalized (dimensionless) parameter $E_\rho o$ can be written:

$$E_\rho o = \frac{E_\rho}{\left[\frac{-I \, a \cos \phi}{\pi \sigma_1 d^3} \right]} = \frac{1}{y^3} \left\{ 1 + \int_{1/2}^{\infty} \frac{\left[2 - \left(\frac{2x}{y} \right)^2 \right] a^x}{\left[1 + \left(\frac{2x}{y} \right)^2 \right]^{5/2}} \, dx \right\} \quad \text{(Eq. 13)}$$

The asymptotes can be found from previous equations.

At short ranges, $E\rho o$ is asymptotic to:

$$E\rho o \bigg| \xrightarrow{\hspace{2cm}} \frac{1}{y^3} \hspace{3cm} \text{(Eq. 14)}$$
$$\bigg|\, r/d \longrightarrow o$$

At long ranges,

$$E\rho o \bigg| \xrightarrow{\hspace{2cm}} \frac{1}{\left(\sigma_2/\sigma_1\right)} \cdot \frac{1}{y^3} \hspace{2cm} \text{(Eq. 15)}$$
$$\bigg|\, r/d \longrightarrow \infty$$
$$\bigg|\, \sigma \neq o$$

When $\sigma_2 = 0$,

$$E\rho o \bigg| \xrightarrow{\hspace{2cm}} 1/2 \cdot \frac{1}{y^2} \hspace{3cm} \text{(Eq. 16)}$$
$$\bigg|\, r/d \longrightarrow \infty$$
$$\bigg|\, \sigma_2 = 0$$

$E\rho o$ was obtained from Equation 13 by numerical integration, using Simpson's Rule. Values were computed for $y = r/d = 1, 2, 5, 10, 20, 50, 100, 200, 500$ for conductivity ratios $(\sigma_2/\sigma_1) = 0, .01, .1,$ and 1. The result is plotted in Figure A1 where smooth curves have been passed through the plotted points. The asymptotes are shown by dashed lines on the graph.
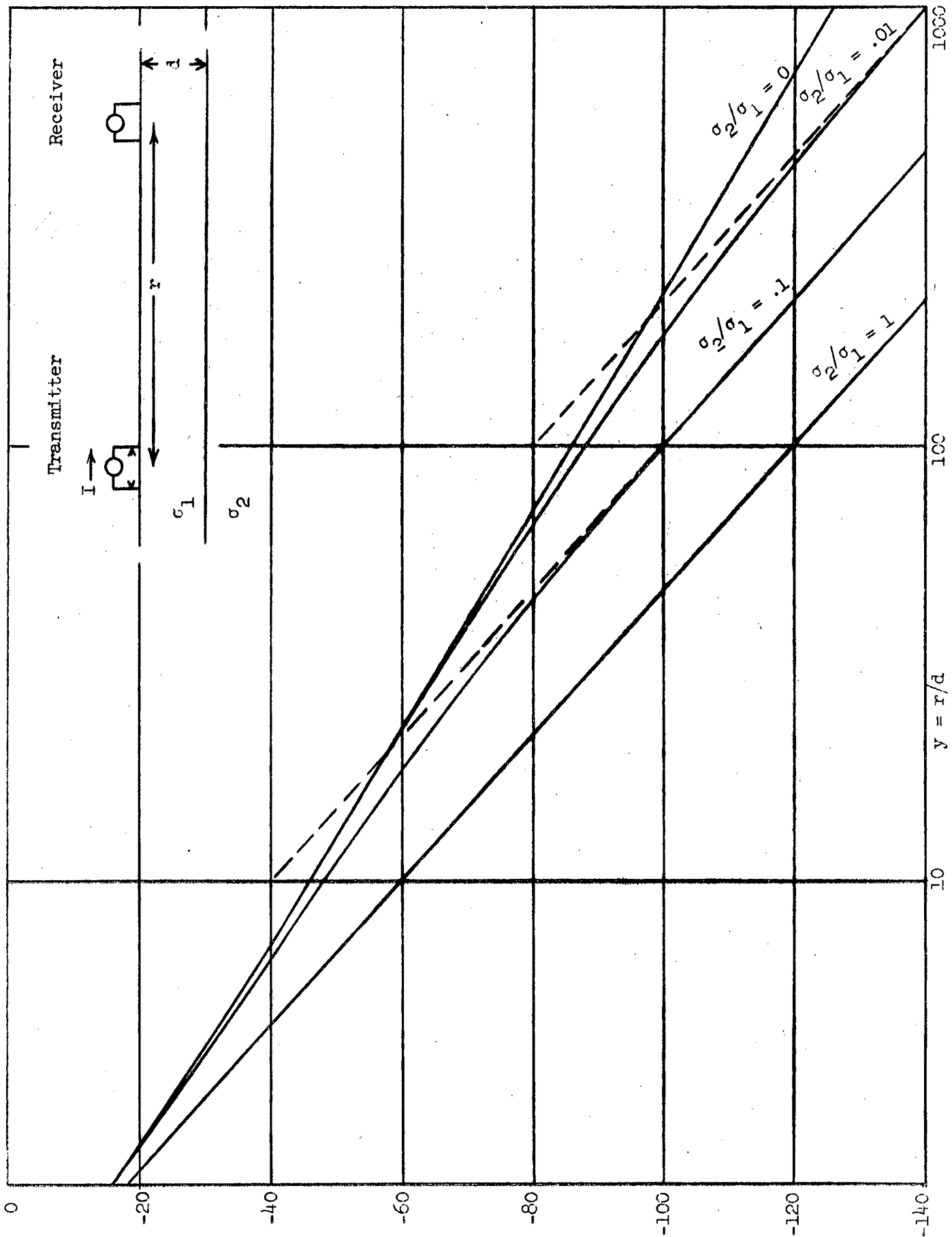
FIGURE A1 . Normalized Radial Component of Electric

(B) Angular Component

The angular component of the electric vector is given by Equation 4 as:

$$E_\phi = \frac{a \sin \phi}{r} \cdot \frac{dV}{dr}$$

$$= -\left[\frac{Ia \sin \phi}{\pi \sigma_1 d^3}\right] \cdot \frac{1}{2y^3} \left\{ 1 + 2 \int_{1/2}^{\infty} \frac{a^x}{\left[1 + \left(\frac{2x}{y}\right)^2\right]^{3/2}} dx \right\}$$

(Eq. 17)

A normalized parameter $E\phi o$ can be written:

$$E_{\phi o} = \frac{E_\phi}{\left[\frac{-Ia \sin \phi}{\pi \sigma_1 d^3}\right]} = \frac{1}{2y^3} \left\{ 1 + 2 \int_{1/2}^{\infty} \frac{a^x}{\left[1 + \left(\frac{2x}{y}\right)^2\right]^{3/2}} \right\}$$

(Eq. 18)

The asymptotes can be found from the equations previously supplied. Thus, at short ranges, $E_{\phi o}$ is asymptotic to:

$$E_{\phi o} \Big|_{r/d \longrightarrow o} \longrightarrow \frac{1}{2y^3}$$

(Eq. 19)

At long ranges,

$$E_{\phi o} \Big|_{\substack{r/d \longrightarrow \infty \\ \sigma_2 \neq 0}} \longrightarrow \frac{1}{\sigma_2/\sigma_1} \cdot \frac{1}{2y^3}$$

(Eq. 20)

When $\sigma_2 = 0$,

$$
\left. E_{\phi o} \right| \qquad \longrightarrow \qquad \frac{1}{2y^2}
$$

$$
r/d \longrightarrow \infty
$$

$$
\sigma_2 = 0
$$

(Eq. 21)

$E_{\phi o}$ can be computed from Equation 18 by numerical integration. This has been done, and a plot is given in Figure A2, on which the asymptotes are shown by dashed lines.

(C) An Approximate "Break Point" Analysis

Equation 9 for the potential due to a monopole was obtained by approximating the discrete image current source distribution by a single discrete current source at the surface, and a continuous distribution extending from a depth d downward. Alternately, a continuous current distribution extending over the complete range from depths o to oo may be considered. In this case, the continuous linear current source density q (D) at depth D is given by:

$$
q(D) \; = \; \frac{I}{d} \; \alpha^{D/2d} \; = \; \frac{I}{d} \; e^{D/2d \, \ln\alpha} \qquad o \leqslant D \leqslant \infty \tag{Eq. 22}
$$

A "depth of penetration" can be defined by

$$
\delta \; = \; - \; \frac{2d}{\ln\alpha} \tag{Eq. 23}
$$

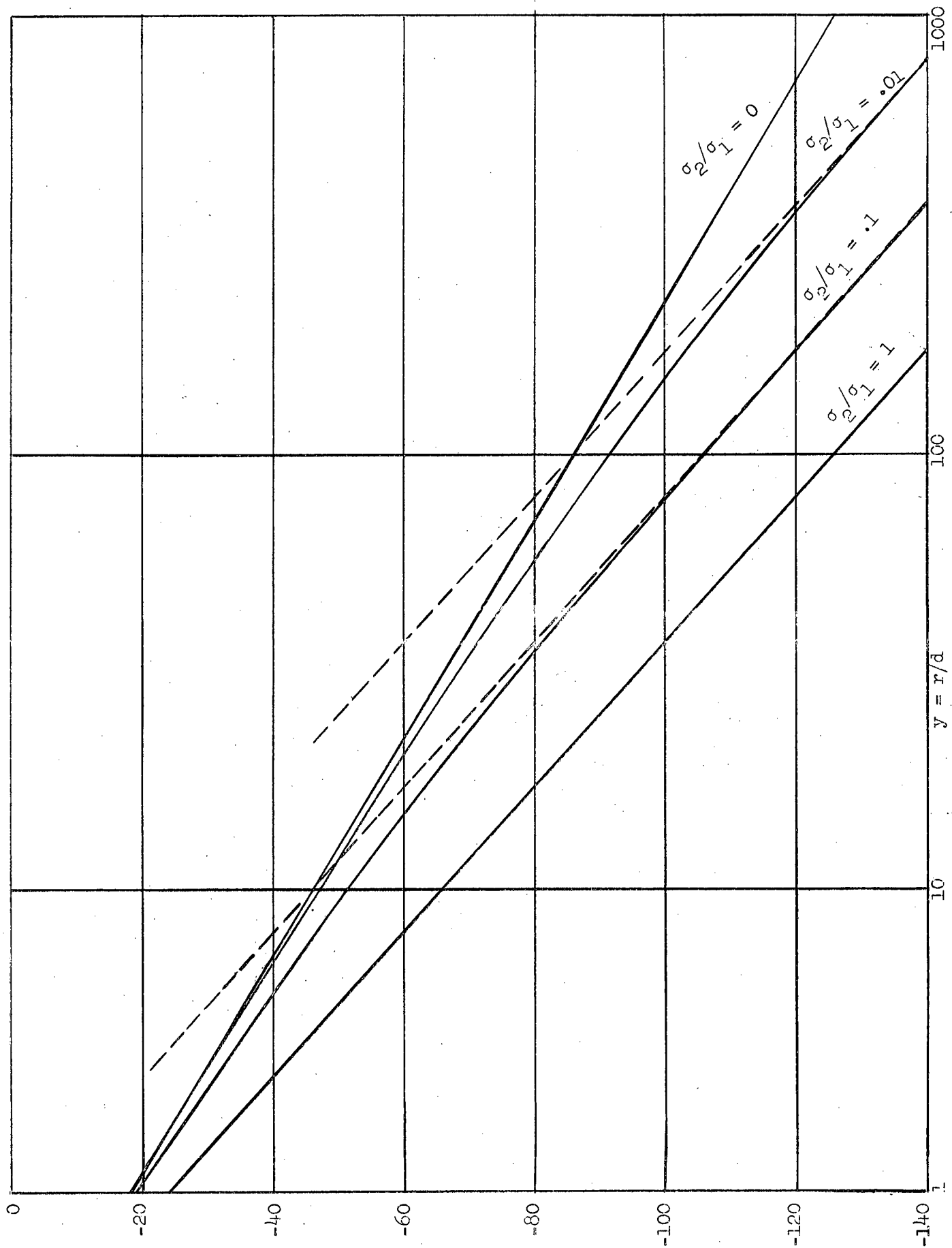which is the depth at which $q(D) = \frac{1}{e} \, q(o)$.

50X1

FIGURE A2. Normalized Angular Component of Electric Vector E,

Then it is reasonable to assume that beyond some range $(R_0 \cong \xi \delta)$ the potential will be approximately proportional to inverse range as if there were a single discrete current source. Beyond this range the electric vector from a current dipole would be proportional to inverse range cubed.

Thus,

$$R_0 \cong \frac{2d\,\xi}{\ln\alpha} \qquad\qquad (Eq. 24)$$

and

$$\alpha \cong e^{-\frac{2d\,\xi}{R_0}} \qquad\qquad (Eq. 25)$$

The normalized range (R_0/d) corresponds, in Figures 6 and 7 to the break point where the asymptote for E_0 crosses the asymptote for E_0

$$\left| \begin{array}{l} r/d \longrightarrow \infty \\ \sigma_2 \neq 0 \end{array} \right. \qquad\qquad \left| \begin{array}{l} r/d \longrightarrow \infty \\ \sigma_2 = 0 \end{array} \right.$$

From Figure A1, or from Equations (15) and (16), it can be seen that the break point for $E\rho$ occurs at normalized range

$$y_0 = \frac{R_0}{d} = \frac{2}{(\sigma_2/\sigma_1)} \qquad\qquad (Eq. 26)$$

From Equations (24) and (26),

$$\xi\rho = \frac{-\ln\alpha}{\sigma_2/\sigma_1} \qquad\qquad (Eq. 27)$$

Since $-\ln\alpha \cong 2\frac{\sigma_2}{\sigma_1}$ (for $\sigma_2/\sigma_1 \ll 1$), then $\xi\rho \cong 2$.

Similarly, the break point for E_ϕ occurs at normalized range

$$y_0 = \frac{1}{(\sigma_2/\sigma_1)} \qquad\qquad (Eq. 28)$$

and

$$\xi_\phi \cong 1.$$

50X1

The break points for $E\rho$ and E_ϕ, given by Equations (26) and (28), are plotted as a function of σ_2/σ_1 in Figure A3.

V. Discussion

At very short ranges (i.e. $y = r/d \ll 1$), the variation of the electric vector is inversely proportional to the cube of range, the maximum radial component (for $\phi = 0$) being twice that of the maximum angular component ($\phi = 90°$). This situation extends to all ranges when $\sigma_2 = \sigma_1$.

For $\sigma_2 < \sigma_1$, which is the case of interest here the variation in electric vector quickly approaches the intermediate "asymptote" $\frac{1}{2y^2}$ for the maximum of either the radial or the angular component.

Thus, in these intermediate ranges, the maximum radial component equals the maximum angular component. Finally, another break point is reached (provided $\sigma_2 \neq 0$) after which the variation is again inverse cubed with range. In this final asymptotic region, however, the break points are such that the maximum of the radial component (i.e. for $\phi = 0$) is twice the maximum of the angular component (for $\phi = 90°$). Thus, at long ranges the "end-fire" signal is 6 db greater than the "broadside" signal.

In either event, the presence of the base complex of conductivity σ_2 (where $\sigma_2 < \sigma_1$) results in a signal enhancement of (σ_1/σ_2). For example, if $\sigma_2/\sigma_1 = 0.1$, then $\sigma_1/\sigma_2 = 10$, and a 20 db improvement results.

VI. Experimental Measurements and Fitting of Measured Data

The curves in Figures A1 and A2 can readily be used to test the model against experimental results. Suppose that $E\rho$ and E_ϕ are sets of measured values of the radial and angular electric vector. Then the normalized quantities $E\rho_o$ and $E_{\phi o}$ can be expressed, from Equations (13) and (18), as:

$$E\rho_o = \left[\frac{\pi \sigma_1 d^3}{-I \, a \, \cos\phi}\right] E\rho \qquad\qquad (Eq. 29)$$
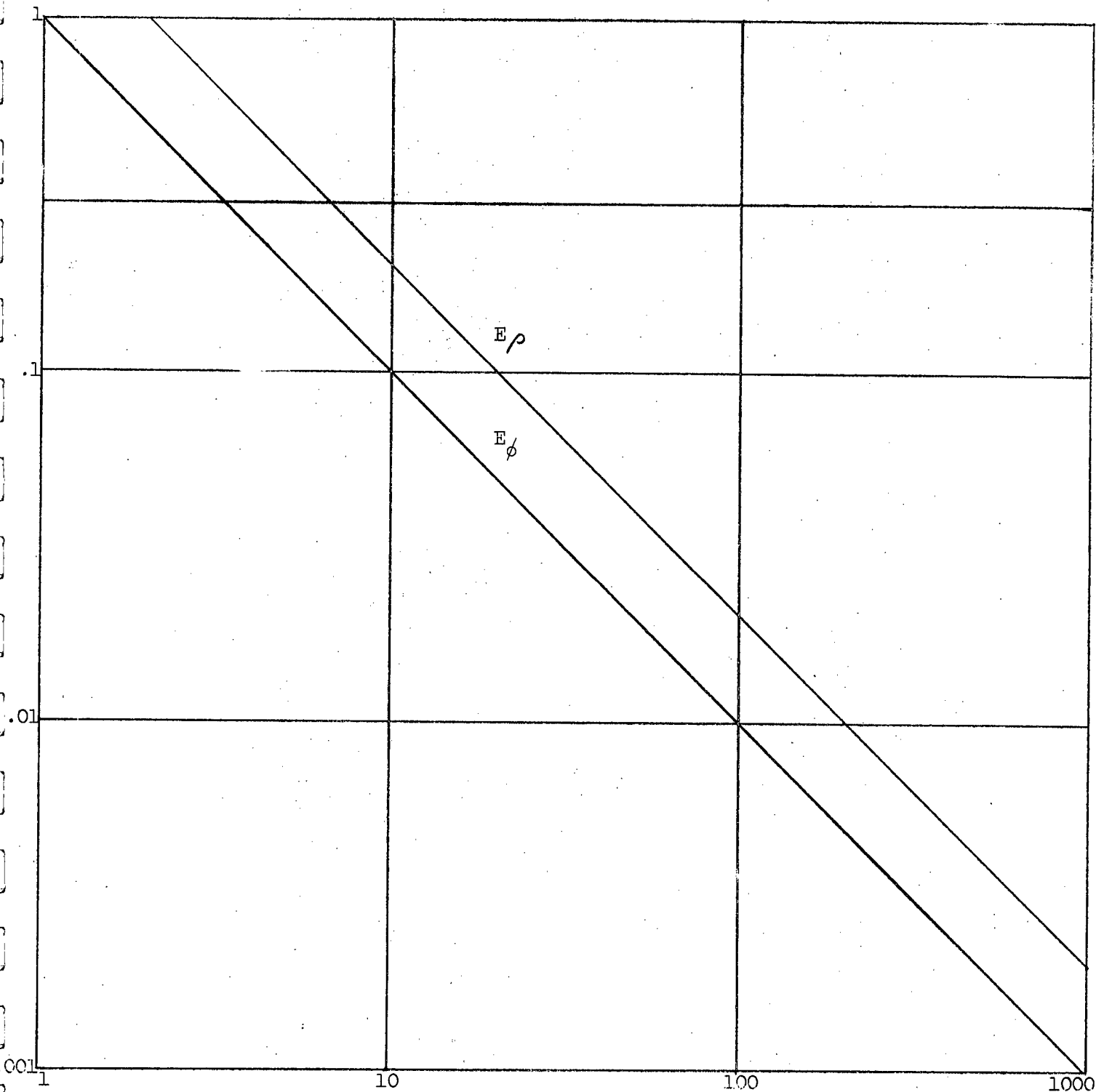
FIGURE A3. Break Point $y_o = R_o/d$ vs. Conductivity Ratio σ_2/σ_1

and

$$E_{\phi o} = \left[\pi \frac{\sigma_1 d^3}{-I \, a \, \sin \phi}\right] E_\phi \qquad \text{(Eq. 30)}$$

Then numerical values for $E\rho_o$ and $E_{\phi o}$ can be computed using assumed (or known) values for σ_1 and d, and the results plotted on Figures A2 and A3.

If the plotted points do not fall along one of the family of lines in the graph, the plot may be translated in an attempt to fit it to one of the curves, by varying σ_1, or d, or both. Varying σ_1 merely shifts the point up or down, with r/d remaining constant. When d is varied, the point moves along an inverse cube line. The effect of making such variations is illustrated in Figure A3. In this Figure, a point A is shown translated into several positions B, C, D along the curve for $(\sigma_2/\sigma_1) = .01$. In a similar way, a given point may be translated anywhere along any curve. All other points must, of course, be equally translated. The point-to-point translation is unique in terms of d and σ_1, and in principle, if the layered-earth assumption actually exists, then a set of measured points is translatable to fit a unique (σ_2/σ_1) curve. Thus, suppose that is is known that the single-layer condition exists, but d, σ_1 and σ_2 are unknown. Then several measured values of $E\rho$, for example, measured at several ranges suffice in principle to uniquely determine d, σ_1, and σ_2. A somewhat similar procedure is used in geophysical prospecting. In actual practice, a set of measured data will fit the curves given here only if the actual earth conductivity profile is reasonably approximated by the single-layered model assumed.

If an approximate break point is evident from raw measured data and either σ_2/σ_1 or d is known, the unknown quantity can be approximated directly by use of Figure A4.
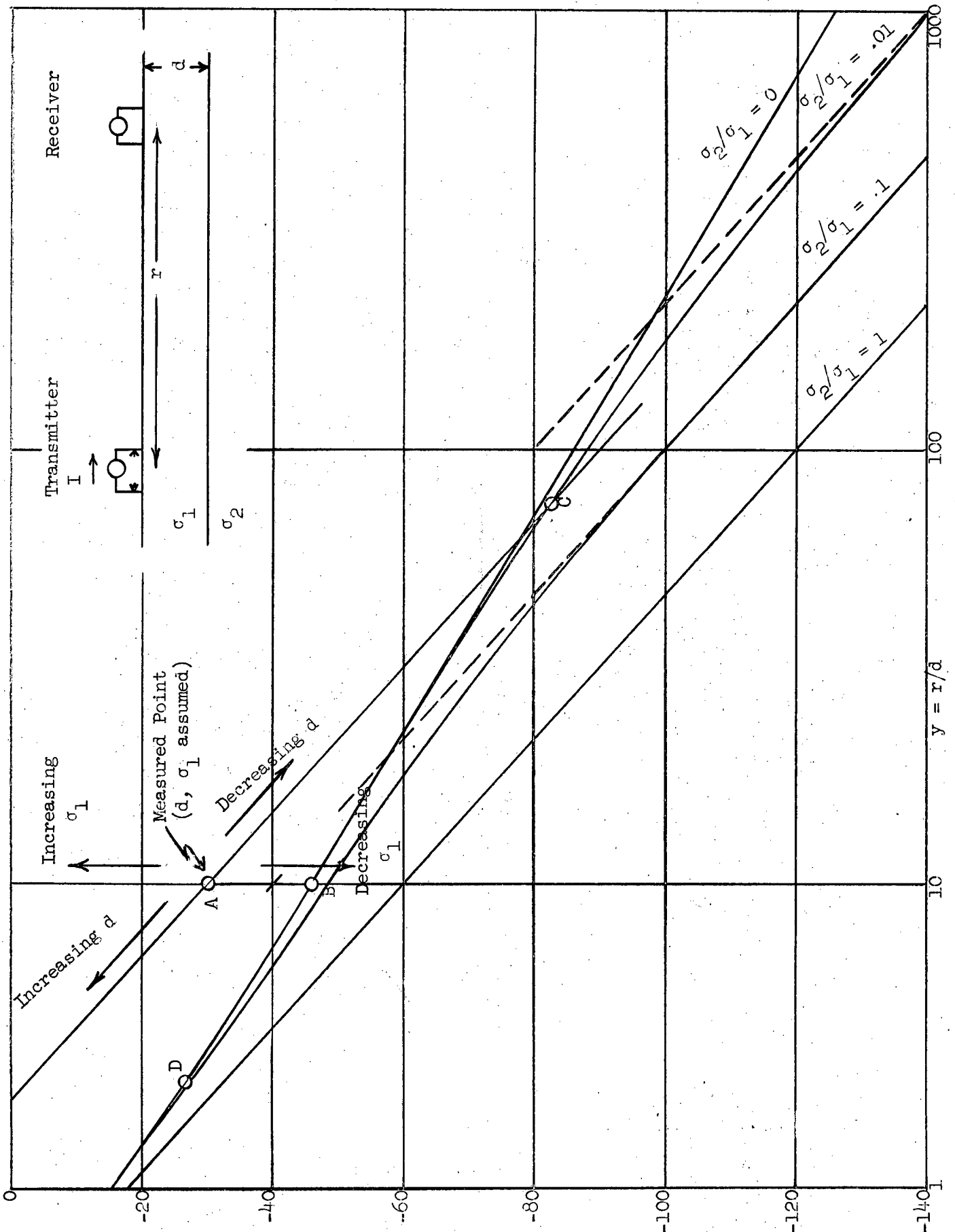
FIGURE A4. Fitting of Measured Points

APPENDIX B

ULTRA LOW FREQUENCY FIELD TESTS AT 1/2 CYCLE PER SECOND

ULTRA LOW FREQUENCY FIELD TESTS AT 1/2 CYCLE PER SECOND

has recently conducted field measurements 50X1
of signal strength at a frequency of 1/2 cps to verify the effect of surface
conducting layers. The tests were conducted using the Company's transmitter
facility in the Mojave desert. Geophysical surveys of the area had shown a
surface conductivity of about 0.05 mho/meter, and a surface layer depth of
about 600 meters. Conductivity of the quartz monzonite basement material was
unknown, but would be expected to be considerably less than that of the surface
material. Three measurements of E_ϕ, and one of $E\rho$ were taken, at different
ranges. The data are summarized in Table IB. The results shown good agreement
with the theoretical predictions. In particular, the data are an excellent fit
for the theoretical curves corresponding to σ_2/σ_1 = 0.1, as shown in the plot
of Figure B1. This implies a lower conductivity of about 0.005 mho/meter, which
would be expected for this quartz monzonite basement.

50X1

TABLE IB

COMPUTATION OF NORMALIZED ELECTRONIC FIELD STRENGTH FOR 1/2 CYCLE PER SECOND TEST

Receiver Site No.	Range in Kilometers	$y = \frac{r}{d}$	Location	Received Signal μv/meter RMS	Normalized Signal* $E\rho o$ or $E\phi o$ in db
1	3.62	6.03	NW Broadside (Eϕ)	62.5	-42.9
2	6.84	11.4	NW Broadside (Eϕ)	18.6	-53.4
3	12.8	21.3	NW Broadside (Eϕ)	3.3	-68.4
4	67.6	112.7	SW End-On (Eρ)	0.07	-101.9

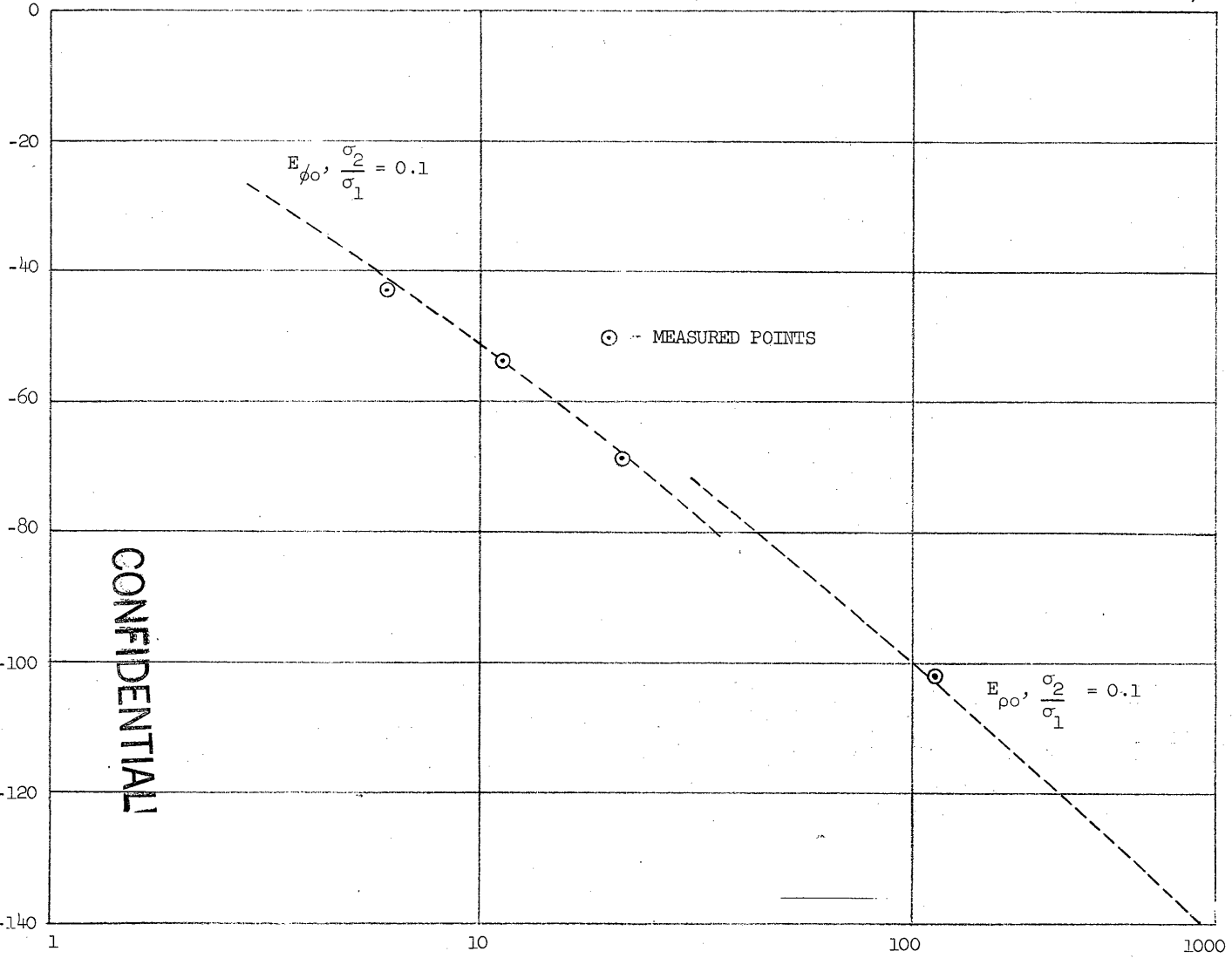Values used in computation: σ_1 = 0.05 mho/meter (average from geophysical measurements)

d = 600 meters (average taken from geological survey data)

Transmitter electrode spacing 1137 meters.

Transmitter current 260 amps RMS.

*cf. Appendix A.

50X1

FIGURE B1.   ONE-HALF CYCLE PER SECOND TEST OVER LAND (COMPARISON OF MEASURED AND THEORETICAL VALUES)

$E_{\phi o}, \dfrac{\sigma_2}{\sigma_1} = 0.1$

$\odot$ -- MEASURED POINTS

$E_{\rho o}, \dfrac{\sigma_2}{\sigma_1} = 0.1$

CONFIDENTIAL

CONFIDENTIAL

Page B-4

NORMALIZED RANGE $y = r$